Comparative Analysis of the Stage-Discharge Rating Operated in Gradual Varied Flows with Alternative Streamflow Monitoring Approaches

M. Muste[1], *K. Kim[1,2], D. Kim[2], I. Demir[3,4]

[1]IIHR–Hydroscience & Engineering, University of Iowa, Iowa City, Iowa, USA.

[2]Civil & Environmental Engineering, Dankook University, Yongin, Gyeonggi, South Korea.

[3]Department of River-Coastal Science and Eng, Tulane University, New Orleans, LA, USA.

[4]ByWater Institute, Tulane University, New Orleans, LA, USA.

*Corresponding author: Kyeongdong Kim (kyeongdong-kim@uiowa.edu)

Keywords

- Streamflow monitoring, stage-discharge rating, index-velocity method, slope-area method; gradually varied flows, hysteresis

Key Points

- Streamflow data reported by stage-discharge ratings during gradually varied flow are often exceeding the 5% uncertainty allowed for streamflow time series.
- Correction applied to stage-discharge rating reconstruct the traces of the hydraulic variable in gradually varied flow with high confidence.
- Use of multi-variate monitoring methods offers a reliable alternative for providing more accurate time series during gradually varied flows.
- Inclusion of free-surface slope and channel cross-section into the monitoring protocols facilitates the understanding of local issues at gaging stations.

Abstract

Streamflow data derived from stage-discharge rating curves (HQRC) are reported without uncertainty compelling users to treat them as absolute and deterministic. However, ignoring uncertainty is no longer viable, as data users increasingly demand confidence in measurements - especially for cross-agency comparisons and scientific or legal scrutiny. This paper investigates a major factor affecting the accuracy of HQRC data: hysteresis caused by ubiquitous gradually varied flows (GVFs). Although hydrometric agencies apply costly corrections or use other methods to account for this effect on the quality of streamflow mmonitoring data, assessing their effectiveness is challenging and largely unknown. Consequently, most HQRC stations operate without accounting for hysteresis-induced error. Motivated by the lack of comparisons between data produced during GVFs by HQRC, HQRC corrections, and multi-variate monitoring methods, this paper evaluates the performance of several methods from each category applied

to a range of flows at three gaging stations. Besides quantifying the HQRC uncertainty, we provide guidelines to properly account for it.

1 Introduction

Streamflow time series reported by hydrometric agencies serve as foundational datasets for both practical applications and scientific research related to rivers and the water cycle (Demir et al., 2022). These data—along with their derivatives, such as annual water budgets and flood frequency analyses—are critical as benchmark datasets for socio-economic and scientific studies on water resource planning, supply management, flood risk assessment (Cikmaz et al., 2025), and streamflow forecasting (Krajewski et al., 2021).

Most gaging stations worldwide (>95%) rely on stage-discharge relationships (HQRCs), a methodology developed in the late 19th and early 20th centuries (Kumar, 2011). HQRCs are site-specific, semi-empirical relationships constructed under assumptions of uniform, steady flow and require detailed knowledge of local hydraulics. They are developed using concurrent stage and discharge measurements, guided by fundamental hydraulic equations, and refined through various statistical and graphical techniques (Kennedy, 1984; Herschy, 2009). After initial development, hydrometric agencies invest substantial effort in adjusting HQRCs over time. Corrections are made through rating extrapolations, temporary or permanent shifts, and manual adjustments based on hydrographers' expertise (overriding). Despite these costly efforts, large-sample studies from Canada, the UK, Norway, and Australia (e.g., Gharari et al., 2024; Coxon et al., 2015; McMahon & Peel, 2019) reveal that reported streamflow data often fail to meet the 5–8% uncertainty targets set by the WMO (2010) and ISO (2020) guidelines, sometimes by significant margins—even when some of the uncertainty sources are excluded from analyses.

Currently, HQRC-derived streamflow data are typically reported without uncertainty estimates, forcing decision-makers and researchers to treat them as absolute and deterministic. However, ignoring streamflow uncertainty is no longer tenable. Data users increasingly demand confidence in measurements, particularly for cross-agency comparisons and scientific or legal scrutiny (McMillan et al., 2017). To assess the impact of subjectivity and variability in streamflow data production, a rigorous and standardized uncertainty analysis (UA) methodology must be applied across all measurement components. Yet, existing UA approaches vary widely in assumptions and protocols, leading to discharge uncertainty estimates ranging from 3% to 200% (Kiang et al., 2018). Key sources of HQRC uncertainty include errors in direct measurements (stage and discharge), limitations in the functional structure of the rating curves (both for the measured and extrapolated ranges), and by neglecting effects of temporal factors altering ratings (short- and long-term influences).

This paper examines one of the most pervasive factors affecting the accuracy of HQRC (stage-discharge rating curve) data: hysteresis caused by gradually varied flows (GVFs). In temperate inland rivers, GVFs can persist for more than 50% of annual flows (Muste et al., 2025). Hysteresis—an inherent feature of these complex flows—introduces loops and phase shifts in the hydrographs of the hydraulic variables during the rise and fall of the flow, phenomena that are not captured by conventional HQRCs due to their reliance on steady-flow assumptions (Henderson, 1966). A USGS study of 5,420 HQRC stations found that 67% exhibited moderate to severe data inaccuracies due to hysteresis (Holmes, 2016). While hydrometric agencies recognize these limitations and apply corrections (Rantz et al., 1982; Kennedy, 1984; Schmidt, 2002; Petersen-Øverleir et al., 2009), assessing their effectiveness remains challenging. The only reliable validation benchmark—continuous direct discharge measurements during flood waves—is seldom available. Given the high costs and unverified accuracy of these corrections, most HQRC stations operate without adjustments, leaving hysteresis-induced errors unaddressed.

Hysteresis severity depends on a dynamic interplay of geomorphic factors (e.g., riverbed slope, sediment mobility, channel/floodplain storage) and hydraulic conditions (e.g., flow rate, channel resistance, downstream controls). These interactions determine whether flood waves develop as kinematic, diffusive, or fully dynamic (Ferrick, 1985; Ponce, 1991; Moussa & Bocquillon, 1996; Moramarco et al., 2008; House et al., 2025a). Each wave produces a distinct hysteretic signature. Crucially, fast-rising floods in low-gradient rivers generate diffusive or dynamic waves, which HQRCs—designed for kinematic waves—cannot accurately represent (Chow, 1959; Henderson, 1966; Herschy, 2009). This limitation poses significant risks for using the simple HQRC data in flood-prone areas, where precise data are vital for forecasting (Xiang et al., 2021), risk assessment and mitigation decisions (Yildirim et al., 2022; Alabbad et al., 2023).

The motivation for this paper stems from the lack of comparisons between the data produced by the simple HQRC rating, the HQRC corrections, and multi-variate monitoring methods during GVFs. The multi-variate term is used to distinguish HQRC, based on only stage measurements, from other monitoring methods that measure additional variables (e.g., index-velocity and free surface slope) besides stage measurements. We evaluate the performance of several methods from each category applied to various fluvial wave magnitudes propagating at three gaging stations. Subsequently, we quantify the HQRC uncertainty due to GVF presence and summarize guidelines to properly account for this uncertainty source.

2 Methods

2.1 Streamflow monitoring methods

Streamflow monitoring protocols have evolved over centuries through incremental advancements that balance available measurement technologies with theoretical understanding of river hydraulics (USGS, 1994). The first developed method, the stage-discharge rating curve (HQRC), requires only stage measurements at a single location - a relatively simple and reliable approach using basic instrumentation through traditional methods and crowdsourced systems (Sermet et al., 2020). By pairing stage records with periodic discharge measurements under the assumption of quasi-steady flow conditions, this method yields semi-empirical rating curves that are both cost-effective and straightforward to implement. While adequate for daily discharge reporting in many applications, this approach proves insufficient for scientific and operational needs requiring sub-daily temporal resolution. A critical example is flood wave propagation, where flow mechanics exhibit substantial hourly variations (Holmes, 2016). Despite this fundamental mismatch with the dynamic nature of river flows, the quasi-steady assumption remains deeply entrenched in global streamflow monitoring practices.

The limitations of the conventional HQRC compared to alternative monitoring methods become apparent by inspecting the Sain-Venant equations governing for GVFs in shallow channels (Muste et al., 2017):

$$\underbrace{\frac{1}{g}\frac{\partial V}{\partial t} + \underbrace{\frac{V}{g}\frac{\partial V}{\partial x} + \underbrace{\frac{\partial H}{\partial x} = \underbrace{S - S_f}_{\textit{kinematic}}}_{\textit{diffusive}}}_{\textit{dynamic quasi-steady}}}_{\textit{dynamic}} \tag{1}$$

where S_0 is the free-surface slope, S_f is the energy (friction slope), H is the water surface elevation (a.k.a., stage) referenced to a local datum, V is the mean cross-sectional velocity, and g is the gravitational acceleration.

The relative contributions of terms in the momentum equation determine the type of fluvial wave observed at a given site. The left-hand side terms representing gravity (S_0) and friction (S_f) forces constitute the kinematic wave component. When $S_0 = S_f$, the wave is purely kinematic - characteristic of steady, uniform flow and dominant in steep-gradient rivers where it accounts for most of the flood wave propagation (Henderson, 1966). The right-hand side introduces additional flow dynamics by accounting for the pressure gradient determined from the free-surface slope (S_w). These three terms generate diffusive waves that account for downstream wave dispersion. The waves are termed as quasi-steady or fully dynamic if the convective and local accelerations are non-negligible in the total momentum budget. The dynamic wave propagates both upstream and downstream relative to the kinematic wave core (House et al, 2025a). Equation (1) reveals that conventional HQRC methods, based solely on kinematic wave assumptions, represent a substantial oversimplification when other momentum terms contribute significantly. Given that derivatives can assume positive and negative values explain why the rising and falling hydrograph limbs exhibit distinct are unique and deviate from the HQRC rating.

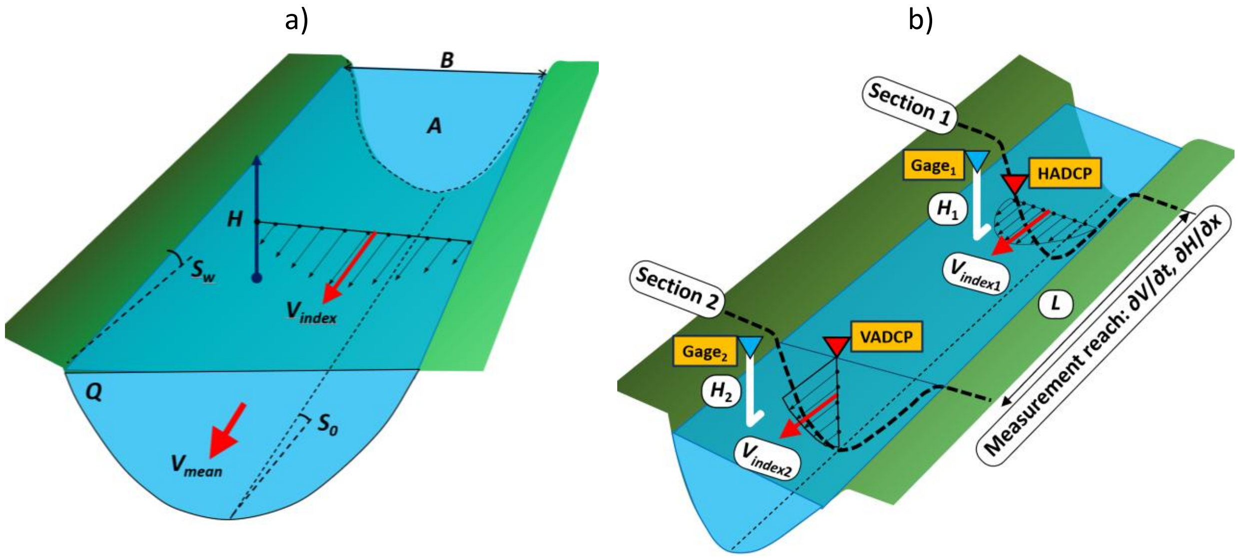

Figure 1. Terminology and instrument arrangements for streamflow monitoring: a) notations; b) instrumentation layout for the acquisition of the variables used by monitoring methods. ***B*** – channel width; ***A*** – cross section area; ***R*** - hydraulic radius; $\boldsymbol{S_w}$ – free-surface slope; $\boldsymbol{V_{index}}$ – index velocity; ***Q*** – discharge (actual); $\boldsymbol{Q_0}$ – discharge (HQRC); ***L*** – spacing between station's cross sections; ***Gage*** – instrument for free-surface elevation measurement; Horizontal ADCP (***HADCP***) and Vertical ADCP (***VADCP***) – instruments for measurement of the index velocity along a horizontal and/or vertical path in the water body.

This section summarizes established approaches for monitoring unsteady flows in the US, focusing on two categories of conventional methods: (1) HQRC correction techniques and (2) multivariate monitoring protocols. Both approaches are well-documented and have been extensively validated through numerous studies. Figure 1b presents the key terminology and instrumentation configurations used for autonomous streamflow monitoring with HQRC alternative methods. The figure illustrates that multiple instrument types can measure each primary hydraulic variable, with some devices (e.g., Acoustic Doppler Current Profilers, ADCPs) capable of simultaneously capturing multiple variables through integrated sensor packages. Table 1 provides a concise overview of the mathematical formulations governing these alternative monitoring methods, including their respective wave-type applicability ranges.

The stage-discharge rating (HQRC). The HQRC remains the most widely used method for streamflow monitoring since its inception. HQRC development combines fundamental hydraulic equations for steady, uniform flow (Equation 2) with statistical analysis of field discharge measurements collected under various flow conditions (Rantz et al., 1982; Kennedy, 1984). Parameters in Equation (2) take values that reflect the station's hydraulic controls (i.e., local or channel) and the channel geometry for the range of stages at the site. The final rating shape is decided by the direct discharge measurements acquired at the site and typically contains 2-3 manually fitted segments based on the statistical analysis of the discharge measurements and the hydrologists' expert judgement (Rozos et al, 2022). We label the final HQRC rating as Q_0.

HQRC corrections. Hydrometric agencies have long recognized that conventional HQRC ratings are limited in unsteady and non-uniform flow conditions due to their inherent kinematic wave assumption. This assumption considers only gravity and friction terms in the momentum balance (as in Manning's equation for steady flow), neglecting other critical factors present in GVFs (Ponce, 1991). For such flows, the momentum budget must account for additional terms in Equation (1), i.e., the pressure, convective acceleration, and local acceleration term (Ponce, 1991). These terms modify wave behavior, transforming kinematic waves into diffusive, quasi-steady dynamic, or fully dynamic waves (Yen, 1973). Numerous HQRC correction methods have been developed, varying by their assumed wave type and derivation simplifications, all typically applied to the baseline Q_0 rating (e.g., Rantz et al, 1982).

The most commonly applied corrections in USGS practice treat flood waves as diffusive rather than kinematic (Kennedy, 1984). Addressing the backwater effect on HQRCs is made by adjusting the HQRC rating with an empirical stage-fall relationship. The unsteady flow effect addressed by tracking the stage rate-of-change and estimating the wave celerity (Rantz et al., 1982). While operational, these corrections significantly increase costs through additional measurements (e.g., free-surface slope, cross-section area) and computations. The diffusive HQRC corrections offer limited repeatability and reproducibility of the data records due to their weakly-posed scientific basis, non-uniform construction protocols, and the subjective implementation of the rating developers. This study evaluates classical diffusive corrections by Jones (1915) and Boyer (1937) (Equations 3-4 in Table 1).

More robust approaches by Rátky (2000) and Fenton (2001) treat waves as quasi-steady dynamic, retaining all momentum terms except local acceleration - an assumption common in flood routing (Ferrick, 1985). The Rátky (2000) approach (Equation 6), defines wave celerity (c0) as the reciprocal tangent of Q_0 and uses a S_s factor determined from two stage measurements. Rátky (2000) found that this approximative solution shows good agreement with field observations. Fenton's formulation (Equation 8) models flood propagation as an advection-diffusion process that in turn allows to replace the spatial derivative with temporal stage derivatives recorded at one cross section. Fenton (2001) proved with simulations that this approach is accurate within 1% if the two diffusive terms are less than 25% from the total sum.

The most theoretically complete approach considered herein is the Fread (1975) method that treats flood waves as fully dynamic (Equation 10). The implementation of the approach is made by numerical iteration. Recognition of its robustness has led to development of a software package that showed successful deployment at several USGS gaging sites (Domanski et al., 2022; Domanski et al., 2025). Further refinement of the Fread method by Lee & Muste (2017) has been obtained by incorporating detailed cross-section geometry.

The index-velocity method (IVRC). The IVRC has emerged as a robust method for monitoring river reaches affected by backwater and/or unsteady flows, while maintaining accuracy under steady flow conditions (Muste et al., 2019, Muste et al, 2020). The method's revitalization began with the adoption of acoustic technology in the early 1980s, marking a significant advancement from mechanical and electrical current meters to non-intrusive acoustic sensors. This technological evolution has not only improved discharge measurement accuracy but also enabled continuous streamflow monitoring. Addition of an index-velocity to stage results in a better method for tracking GVFs. IVRC implementation requires a cross-sectional survey to develop stage-area rating (HARC). Similarly to HQRC, discharge and stage measurements are simultaneously acquired to establish index-velocity vs. mean velocity relationship (IVRC rating). This rating is simpler to construct compared to HQRC as it is obtained with only statistical regression (Levesque & Oberg, 2012). The final discharge time series is computed as the product of area from HARC and the mean velocity derived from index-velocity ratings. Notably, IVRC ratings are developed without distinguishing between rising and falling hydrograph limbs, which maybe questionable for sites with significant hysteresis (Muste et al., 2022a).

Continuous Slope-Area method (CSA). The recent availability of low-cost pressure transducers has enabled renewed application of the slope-area (SA) method for continuous discharge measurement (Smith et al., 2010; Stewart et al., 2012). Building on the original SA developed to extend HQRC ratings for high-flow conditions (Dalrymple & Benson, 1967), the Continuous SA (CSA) method substitutes bed slope (S_0) with the free-surface slope (S_w) in Equation (11). Deploying pressure sensors at multiple stations (minimum three recommended), the CSA has been successfully tested for monitoring steady and unsteady flows by these authors in small streams (Muste et al., 2016; Lee & Muste, 2017; Muste et al., 2019) and large rivers (Muste et al., 2025). The method is only applicable to short river reaches (< 5 channel widths). Using excessively long reaches might include natural flow changes (e.g. bed slope breaks, bends, tributary inflows) that can lead to significant errors in the free-surface slope estimation (Schmidt & Garcia, 2003; House et al., 2025b).

Table 1. Essential specifications for the HQRC alternative methods analyzed in the study

Method (assumed wave type)	Code	Input measurements & site specifications: Arrangement	Variable(s) & parameters	Cross-sections	Monitored output, *Q(t)*, based on:
Stage-discharge *(kinematic wave)*	Q_0	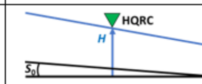	H	1	HQRC (**Q_0**) semi-empirical rating guided by: $Q_0 = a(H - H_0)^b$ (2) *a*, *b* coefficients accounting for station control
Corrected stage-discharge – Jones (1915) (*diffusive wave*)	Q_{JON}	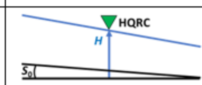	H & Q_0, $A(H)$, S_0	1	HQRC (**Q_0**) semi-empirical rating & $Q = Q_0\left[1 + \frac{1}{S_0 c_0}\frac{\partial H}{\partial t}\right]^{\frac{1}{2}}$ (3) $c_0 \approx \partial Q_0/\partial A$ (4)
Corrected stage-discharge – Boyer (Rantz et al., 1982) (*diffusive wave*)	Q_{BOY}	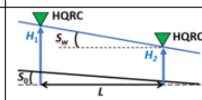	H_1, H_2 & Q_0, $A(H)$, S_0, L	2	HQRC (**Q_0**) semi-empirical rating & $Q = Q_0\left[1 + \frac{1}{S_w c_0}\frac{\partial H}{\partial t}\right]^{\frac{1}{2}}$ (5) & Equation (4)
Corrected stage-discharge – Rátky (2000) (*dynamic quasi-steady wave*)	Q_{RAT}	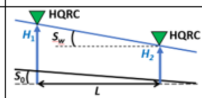	H_1, H_2 & Q_0, $A(H)$, $B(H)$, S_0, L	2	$Q = Q_0\left[1 + \frac{1}{c_0\sqrt{S_s}}\frac{\partial H}{\partial t} - \frac{Q_0}{2Bc_0S_s}\frac{\partial^2 H}{\partial x^2}\right]^{\frac{1}{2}}$ (6) & Equation (3); $S_s = S_0\,\partial H/\partial x$ (7)
Corrected stage-discharge – Fenton (2001) (*dynamic quasi-steady wave*)	Q_{FEN}	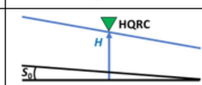	H & Q_0, $A(H)$, $B(H)$, S_0	1	$Q = Q_0\left[1 + \frac{1}{2}\frac{1}{c_0 S_0}\frac{\partial H}{\partial t} - \frac{1}{2}\frac{D}{c_0^3 S_0}\frac{\partial^2 H}{\partial t^2}\right]$ (8) & Equation (4); $D = Q_0/2BS_0$ (9)
Corrected stage-discharge – Fread (1975) (*dynamic wave*)	Q_{FRE}	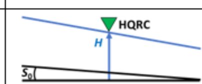	H & Q_0, $A(H)$, $B(H)$, S_0, n	1	$Q - \frac{AR^{\frac{2}{3}}}{n}\left[S_0 + \frac{A}{KQ}\frac{\partial H}{\partial t} + \frac{Q}{gA^2}\left(\frac{\partial A}{\partial t} - \frac{B}{K}\frac{\partial H}{\partial t}\right) + \left(\frac{\frac{Q'}{A'} - \frac{Q}{A}}{g\Delta t}\right)\right] = 0$ (10)
Index-velocity *(diffusive wave)*	Q_{IVRC}	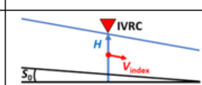	H, *IVRC* & $A(H)$	1	Q (t) time series
Continuous slope-area ***(no rating curves)*** *(diffusive wave)*	Q_{CSA}	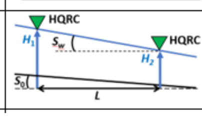	H_1, H_2 & $A(H)$, n, L	2	$Q = \frac{1}{n}AR^{2/3}S_w^{1/2}$ [SI units] (11) *n* – Manning's roughness coefficient

Ensuing from the summary provided in Table 1 is that the methods ***Q_{JON}***, ***Q_{BOY}***, ***Q_{RAT}***, ***Q_{FEN}***, and ***Q_{FRE}*** require the availability of a simple HQRC rating curve (Q_0) for the station. The methods ***Q_{BOY}***, ***Q_{RAT}***, and ***Q_{CSA}*** require continuous measurement of stage at two locations for determining the free-surface slope (FSS). The only method that requires continuous index-velocity measurements (and the index-velocity rating) is ***Q_{IVRC}***. The steady-state stage-discharge (Q_0) can be obtained from: a) an existing rating or b) using Equation (11) with actual data for cross-section and known values for the bed slope and Manning's n. If one adopts the first approach, the method can be considered a correction for Q_0 (e.g., Schmidt & Garcia, 2003, and Dottori et al., 2009). If the second approach is adopted, simple HQRC is not needed. The FSS ($\partial H/\partial x$ in Equation 1 and Table 1) is determined from stages measured at two closely located cross sections. The Jones and Boyer methods rely on an additional rating curve that relates stage, Q_0 and the second terms in Equations (3) and (4). Some of the HQRC correction methods replace the FSS determined from stage measurements with temporal derivatives of the stage change at one section via the kinematic relationship $(\partial H/\partial x) \cong -/c\ (\partial H/\partial t)$.

2.2 Performance analysis methods

In order to familiarize the reader with the main features of the alternative monitoring performance analysis, this section presents essentials of the one-to-one and one-to-many relationships that characterize the simple HQRC and the alternative monitoring approaches, respectively. Figure 2a illustrates the unique multi-segmented HQRC rating for low, medium, and high flows. This rating is closely dependent on the geometry of the river cross-section overlayed on the same figure. The parameterization and fitting of individual segments are guided by generic hydraulic equations (e.g., steady flows over weirs for low flow and the Manning equation for medium flows). The upper segment of the rating is based on stage-discharge measured pairs, which are quite difficult to obtain. Consequently, the HQRC is often extrapolated. The final shape of the rating is typically obtained through manual fitting of various rating segments. The quality of the final rating is documented using statistical tools applied to the pool of directly measured discharge and stage measurements.

The departure of the traces for HQRC corrections and multi-variate monitoring methods (labeled as Q_{actual} in Figure 2a) from the HQRC rating reveals that flows on the hydrographs rising and falling limbs are driven by different flow mechanisms, as theoretically prescribed by the GVF Equation (1). The non-unique relationship between stage and discharge generated by GVF's is displayed by the looped relationship surrounding the one-to-one HQRC rating (see Figures 2a). The loop in the stage-discharge relationship is a manifestation of hysteresis, which produces non-unique relationships between stage and other hydraulic variables (e.g., energy slope, mean velocity, bed shear velocity, etc.), as substantiated in laboratory studies by Graf & Qu (2004). Conceptual illustrations of these dependencies, as observed through field data, are shown in Figures 2b, 2c, and 2d adapted from Muste et al. (2025). Hysteretic loops are inherently associated with phasing of variable hydrographs, as illustrated in Figure 2e.

The operational implementation of the alternative methods for replacing the simple HQRC involves either acquiring additional measurements for paired variables or using analytical or numerical models for GVFs. The goodness-of-fit validation for these methods is best accomplished by comparing their outcomes with discharge measurements paired with stage measurements acquired throughout the storm event. Such in-situ measurements are rare due to their prohibitive cost and effort. In the absence of direct measurements, we replace the ***Q_{actual}*** data with ***Q_{FRE}***, which replicates the full dynamic wave equation (Fread, 1975).

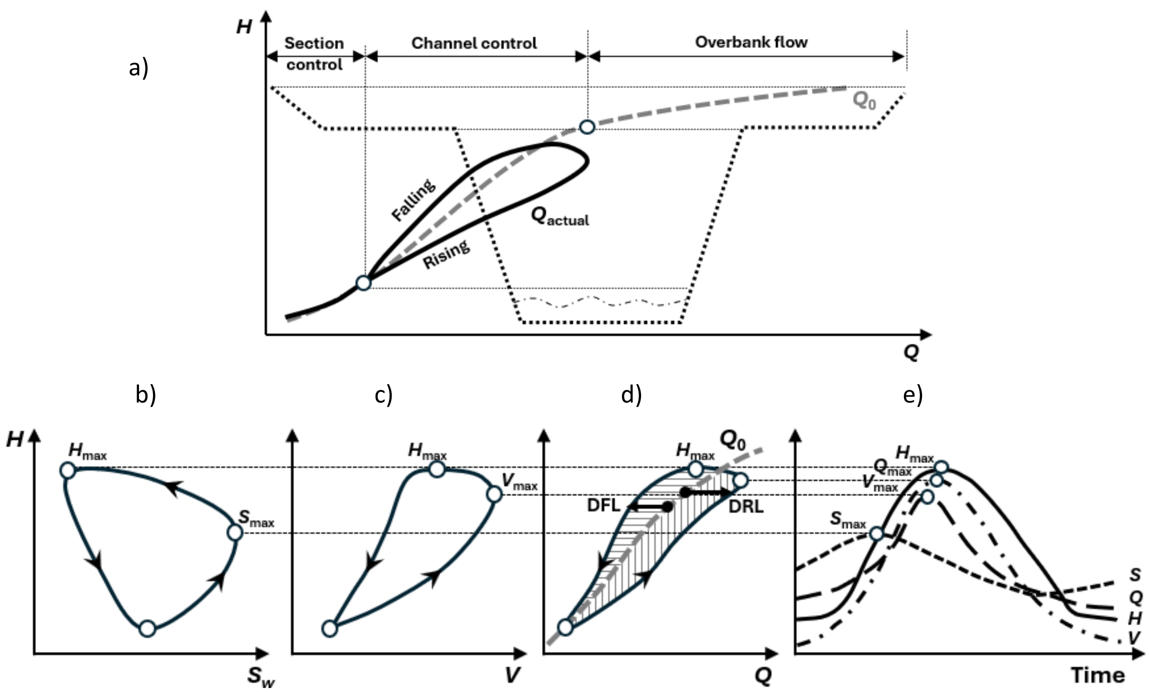

Figure 2. Conceptual illustration of the non-uniqueness of the stage-discharge relationship for gradually varied flows: a) one-to-one ($\boldsymbol{Q_0}$) vs. non-unique stage-discharge relationship ($\boldsymbol{Q_{actual}}$); b), c), d) and e): looped relationships between water surface stage and water surface slope, mean velocity and discharge, respectively. DRL and DFL indicate the departure of actual flows from the HQRC rating on the rising and falling limbs of the hydrograph. e) phasing of the main hydraulic variable hydrographs.

3 Study sites and instrumentation layouts

We evaluated the selected correction algorithms and alternative monitoring methods at three USGS gaging stations representing different river scales: USGS #0233600 on Chattahoochee River at Atlanta, GA (smallest), USGS #0319800 on Kanawha River at Charleston, WV, and USGS #03216070 on Ohio River at Ironton, OH (largest). The key hydraulic characteristics of each site are provided in Table 2. The stations employ distinct monitoring approaches: the Atlanta site is a slope gaging method (Kennedy (1984); the Charleston and Ironton sites are stand-alone IVRC-based gaging stations operated using USGS guidelines (Levesque & Oberg (2012). To enable uniform comparison across sites, we utilized adjacent gaging stations to determine free-surface slope (FSS) at the IVRC locations.

While the index velocity can be acquired using several approaches, i.e., in a point, along a line or at the surface of the water body, the Charleston and Ironton stations are equipped with HADCPs (see Figure 1b). These sites were selected after screening the IVRC stations within the USGS network for the presence of another adjacent station with stage measurement. Such an opportunistic situation allows to estimate the free-surface slope using the stage measurements collected at the neighboring gaging sites. The mean velocity at the Charleson and Ironton are obtained from the stations' index-velocity ratings pairing HADCP measured index-velocities with discharges acquired with moving-boat ADCPs The data at the all USGS gaging stations are collected 15 minute-apart and are publicly available in real time from the open-access site https://waterdata.usgs.gov/nwis/rt. For better substantiation of the analysis features, a 5-point average is applied to the raw data recorded at the stations.

Table 2. Site characteristics and instrumentation for the study sites

Gage site (River)	**Atlanta** (Chattahoochee River, GA)	**Charleston** (Kanawha River, WV)	**Ironton** (Ohio River, OH)
Site & hydraulic specifications	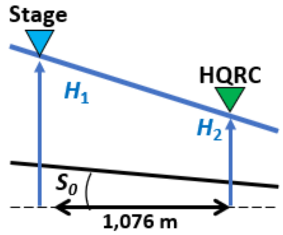	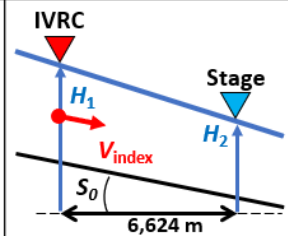	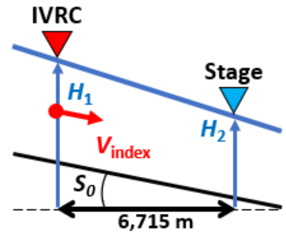
S_0*	**0.0017**	**0.00005**	**0.00001**
B (m)	**50**	**190**	**440**
B / h*	**10/2 = 5**	**190/5 = 38**	**440/10 = 44**
$Q_{min\text{-}max}$ (m^{3}s^{-1})	**≈ 35 – 1158**	**≈ 350 – 4,190**	**≈ 350 – 13,200**
Measurement equipment **	**Stage:** stilling well & float-tape sensor (https://www.usgs.gov/media/images/float-tape-gages) **HQRC stage:** stilling well & float-tape sensor	**IVRC Velocity:** SonTek SL 500 (https://www.xylem.com) **IVRC stage:** SonTek SL 500 **Stage:** FTS SDI-RADAR 26GHz (https://www.environmental-expert.com/products/fts-model-sdi-radar-stage-sensor-737919)	**IVRC Velocity:** SonTek SL 500 **IVRC stage:** SonTek SL 500 **Stage:** YSI WaterLOG H-3611 (https://www.clean.com.br/Menu_produtos/Hidrologia/Medidores_Nivel/H-3611-i_H-3613-i.pdf)

*Determined from measurements at base flow

** Use of trade, firm, or product names is for descriptive purposes only and does not imply endorsement by the authors.

4 Results

A common feature of the site analyses is that the maximum stages for the selected storm events are below the bankful elevation, ensuring strict compliance with the assumptions associated with the equations presented in Table 1. The largest storm analyzed for the Chattahoochee River is an exception, presented here to demonstrate the impact of floodplain flow on the relationships between flow variables. Comparisons are made using both dimensional and non-dimensional graphical representations to enable cross-site inferences on the methods' performance under different influencing factors (e.g., river size, riverbed slope, wave intensities) and to highlight hysteretic features occurring during fluvial wave propagation at the same site. Stage data are referenced to the NAVD 88 datum (www.ngs.noaa.gov/datums). While contrary to best practice (see House et al., 2025b), FSS are determined over relatively large river reach lengths as there were no stations with stage measurements at closer spacing.

The performance of the alternative monitoring methods is evaluated using two quality indicators consistently applied throughout the analysis: a) the deviation of the predicted flows from the HQRC rating (Q_0), when available, and b) the closeness of agreement with a "reference" method deemed to best represent the actual GVFs propagating through the gaging site. For the Charleston and Ironton gaging stations, which do not have established HQRC ratings, we adopted the Fenton (2018) algorithm as a substitute for Q_0. This surrogate, labeled Q_{FEN}, is obtained by applying least-square approximation to all measured data for constructing the index-velocity to mean-velocity rating. The best candidate for the second HQRC quality indicator is obtained by correcting Q_0 data with the Fread (1975) method, labeled Q_{FRE} herein. We chose the Fread method as the best HQRC correction candidate because this algorithm accounts for the full dynamic nature of the propagating wave, as indicated by Equation (10).

USGS #0233600 on Chattahoochee River at Atlanta (GA). The time series analyzed at this gaging site entail three storm events recorded during the 2009-2020 interval illustrated in Figure 3a. Figure 3b represents the maximum stages recorded during these events overlayed on the gage site cross section. It can be noticed that the maximum stages for the small and medium events are below the bankful elevation, while the largest analyzed event exceeds the bankful stage. Figure 3c illustrates the HQRC rating curve developed for this site with the Fenton (2018) method applied to all direct measurements available at the station. As expected, and further discussed in section 5, it can be noticed that the bankful stage produces a discontinuity in the stage-discharge traced by Fread method (i.e., the reference used for representing actual flows).

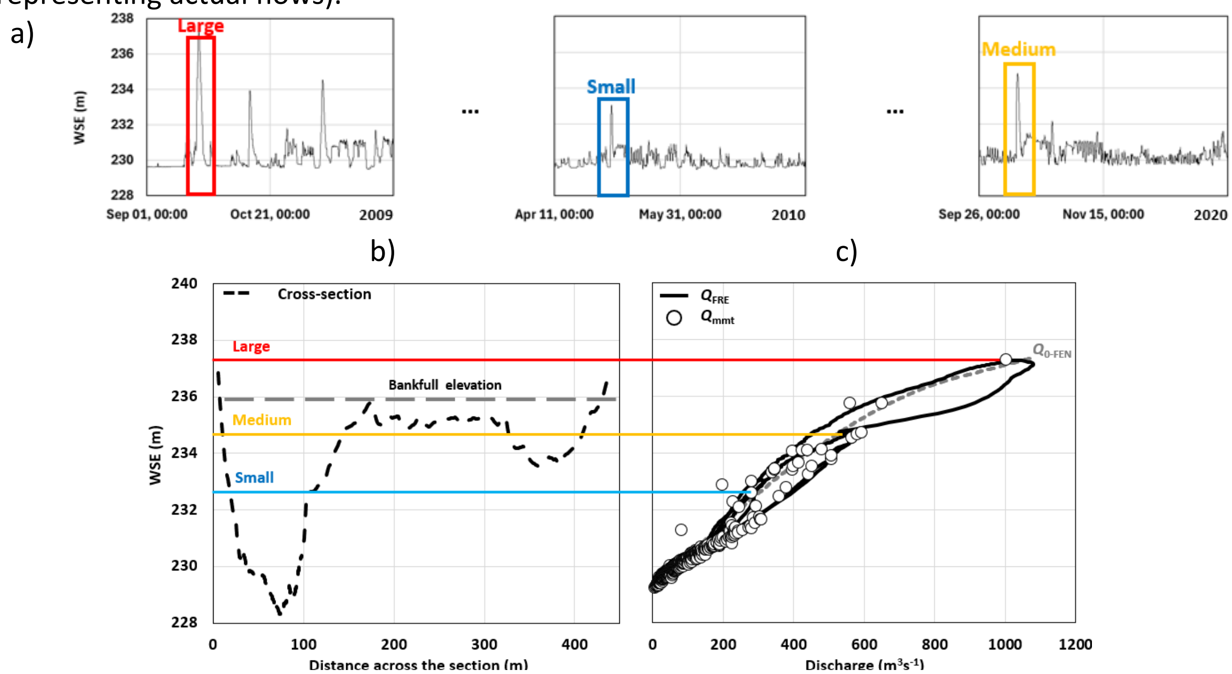

Figure 3. Basic analysis elements for the Chattahoochee station: a) discharge time series for the analysis period; b) river cross-section and maximum stages for the selected events; and c) reference HQRC at the station (***$Q_{0\text{-}FEN}$***) and the trace of the actual flows estimated with ***Q_{FRE}*** correction method

The time-dependent and time-independent graphs of the relationships among the main hydraulic variables for the selected storm events are plotted in dimensional coordinates in Figure 4. The plots in Figures 4a, 4c, and 4e confirm the expected time lag between the stage and FSS peak (see Figure 2). The loops plotted in Figures 4b, 4d, and 4f illustrate the close connection between the magnitude of the phase lag and the looped rating size, and its increase with storm magnitude. It can be also noted that the stage-FSS hysteretic loop is more sensitive to the GVF than the stage-discharge loop and their opposite orientations.

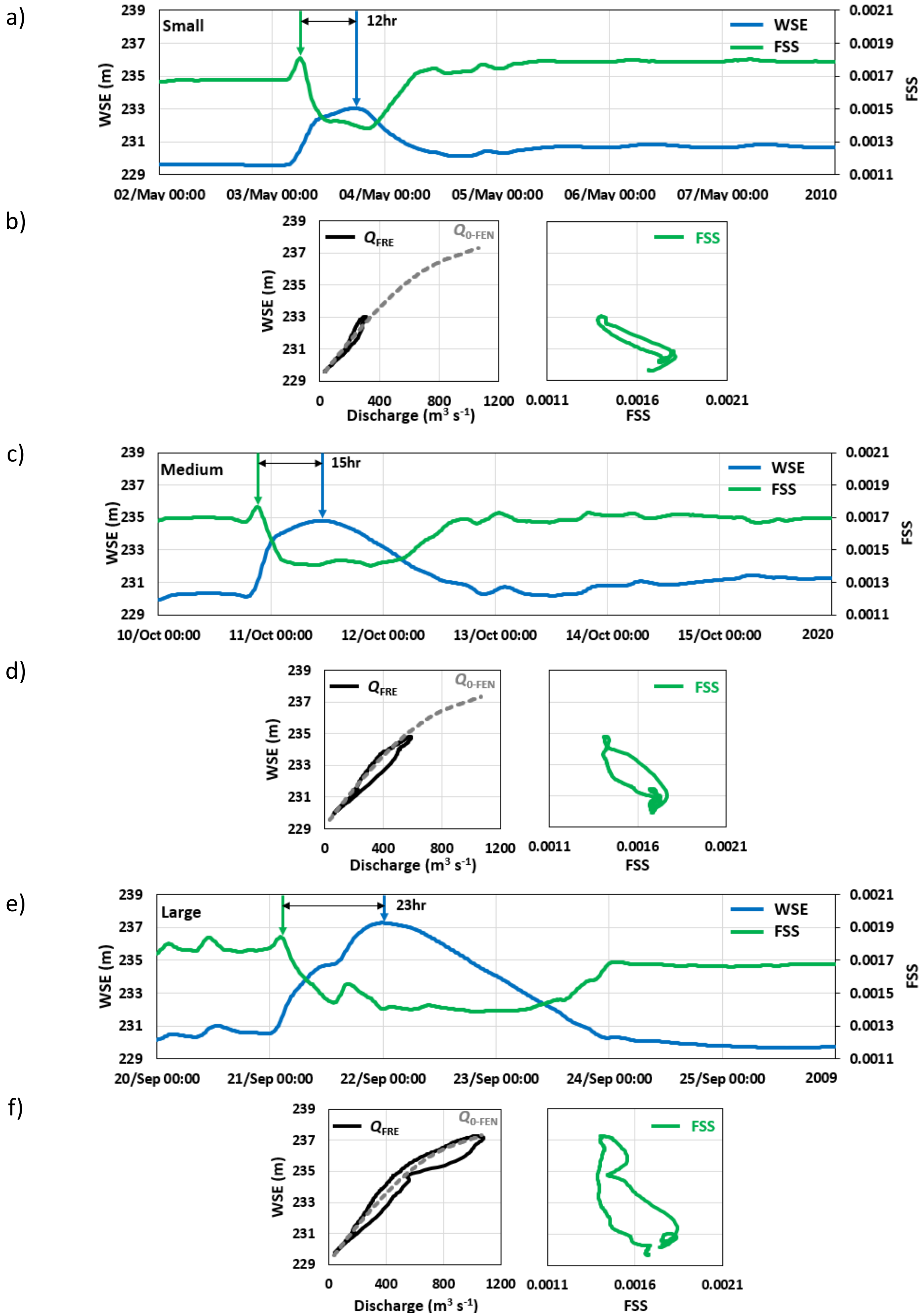

a)
Small
12hr
WSE
FSS
WSE (m)
FSS
239
237
235
233
231
229
0.0021
0.0019
0.0017
0.0015
0.0013
0.0011
02/May 00:00
03/May 00:00
04/May 00:00
05/May 00:00
06/May 00:00
07/May 00:00
2010
b)
Q_{FRE}
$Q_{0\text{-}FEN}$
FSS
WSE (m)
0
400
800
1200
Discharge ($m^3 s^{-1}$)
0.0011
0.0016
0.0021
FSS
c)
Medium
15hr
WSE
FSS
WSE (m)
FSS
10/Oct 00:00
11/Oct 00:00
12/Oct 00:00
13/Oct 00:00
14/Oct 00:00
15/Oct 00:00
2020
d)
Q_{FRE}
$Q_{0\text{-}FEN}$
FSS
WSE (m)
Discharge ($m^3 s^{-1}$)
FSS
e)
Large
23hr
WSE
FSS
WSE (m)
FSS
20/Sep 00:00
21/Sep 00:00
22/Sep 00:00
23/Sep 00:00
24/Sep 00:00
25/Sep 00:00
2009
f)
Q_{FRE}
$Q_{0\text{-}FEN}$
FSS
WSE (m)
Discharge ($m^3 s^{-1}$)
FSS

Figure 4. Dimensional graphs of the: 4a, 4c, 4e time series for the main hydraulic variables for the three storm events identified in Figure 3a; and 4b, 4d, and 4f hysteretic loops between the stage and the main hydraulic variables for the same events.

Figure 5 displays loops in stage-discharge relationships obtained with the correction methods used to adjust the simple HQRC relationship for GVF effects (see Table 1) compared to the unique relationship provided by the simple HQRC rating traced by $\boldsymbol{Q_{0\text{-}FEN}}$. Inspection of Figure 5a shows that all five correction methods recover the dynamic flow features remarkably similar for the falling limb of the hydrographs while displaying slight differences on the rising limb. The results obtained with the Jones methods are similar to those obtained by the study of this site by Petersen-Øverleir (2006). Overall, the corrected loops for the rising limb depart more visibly from the simple HQRC. The discharges produced by the stand-alone slope method at this station, $\boldsymbol{Q_{CSA}}$, are in good agreement with the trace of discharges provided by the $\boldsymbol{Q_{FRE}}$. The hysteresis loops in these plots are visible for stages higher than the bankful stage.

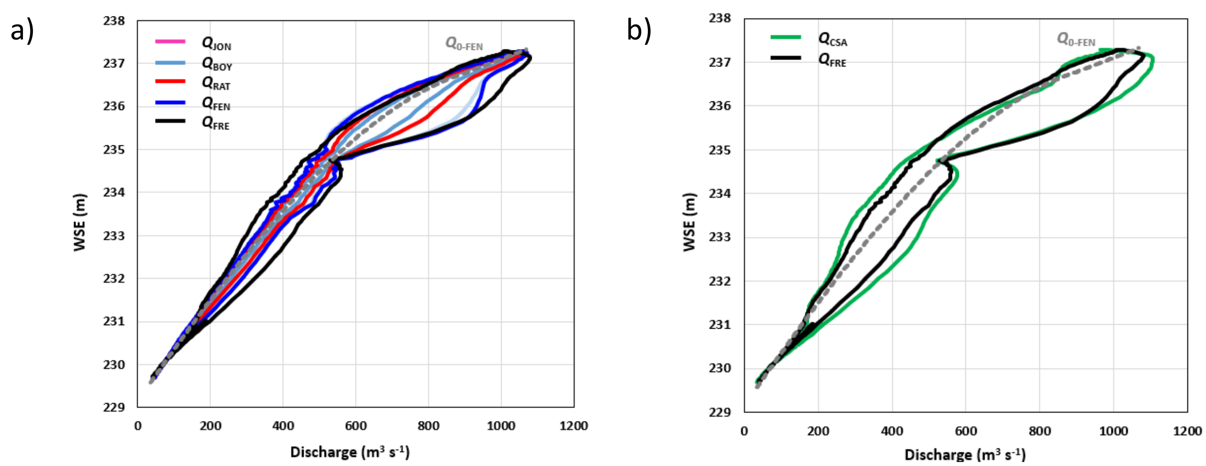

Figure 5. Performance of the alternative monitoring methods at Chattahoochee site for: a) the HQRC correction methods listed in Table 1; and b) the stand-alone CSA method used at the station.

USGS # 0319800 at Charleston (West Virginia). The three storm events analyzed at this site are chosen from data records acquired during the 2020 to 2024 period with the index-velocity and slope methods. Figures 6, 7 and 8 provides the hydrological input, the alternative monitoring methods' performance, and essential hysteretic features using identical formatting and presentation order as for the Chattahoochee gaging station.

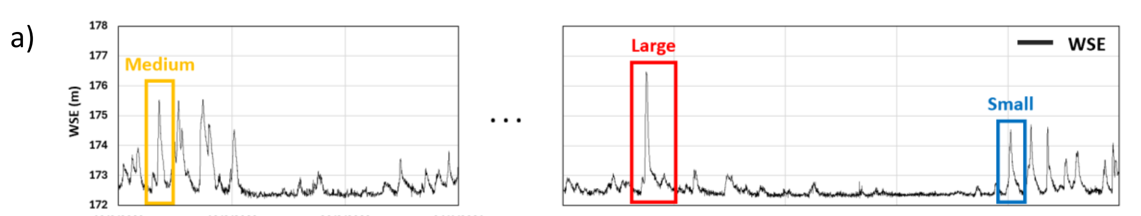

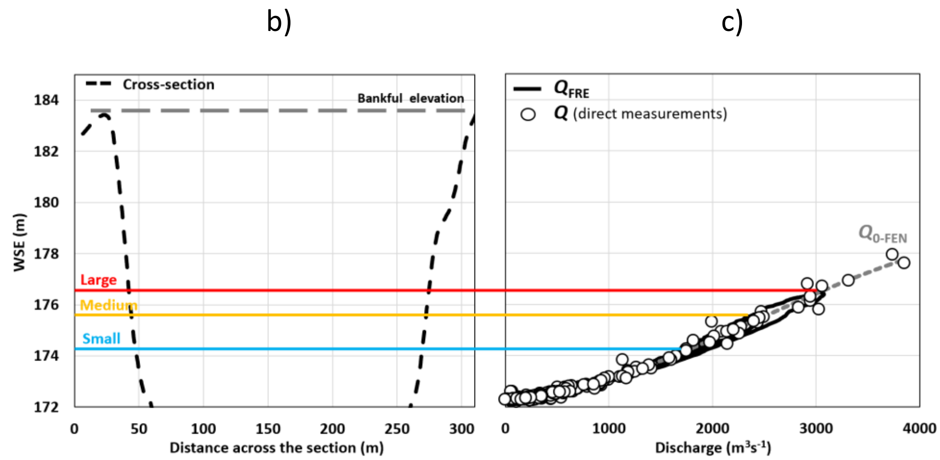

Figure 6. Basic analysis elements for the Charleston station: a) discharge time series for the 2020-2024 period; b) river cross-section and maximum stages for the analyzed events; and c) reference HQRC at the station (***$Q_{0\text{-}FEN}$***) and the trace of the actual flows estimated with ***Q_{FRE}*** correction method.

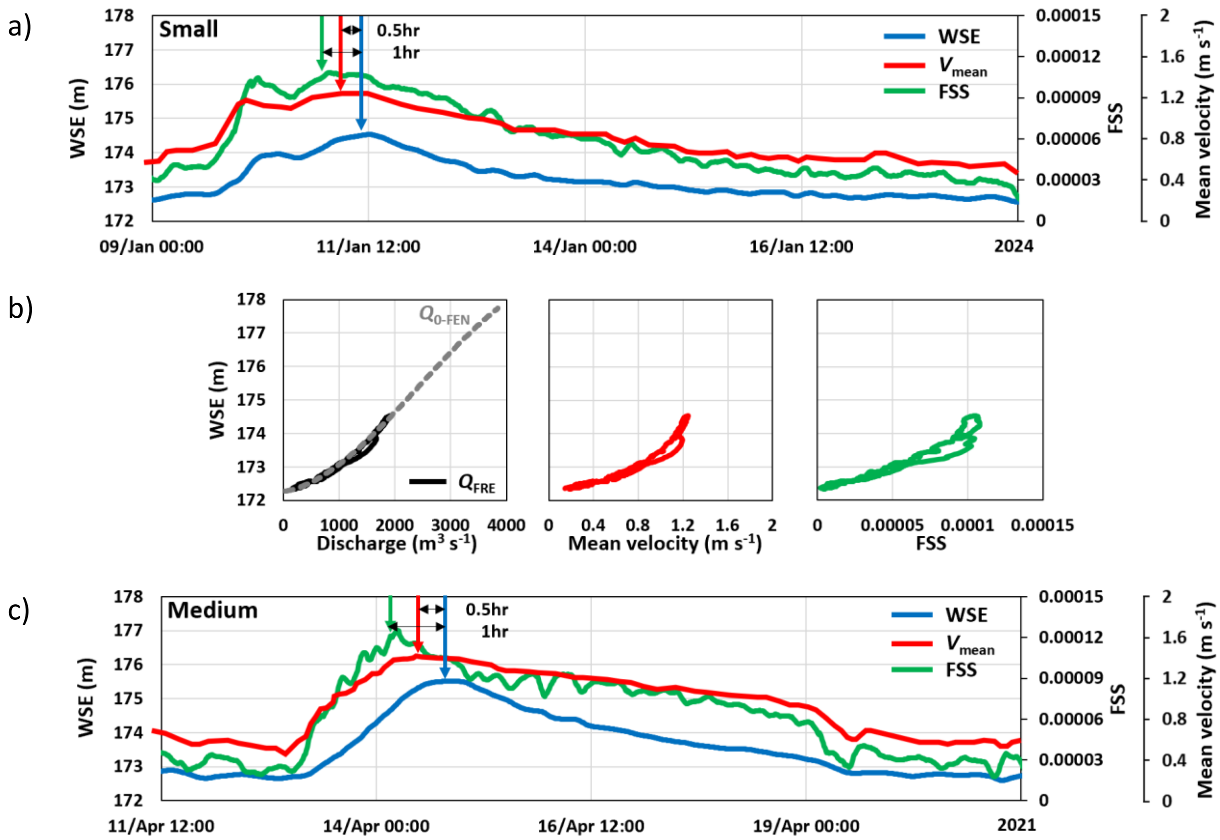

d)

e)

f)

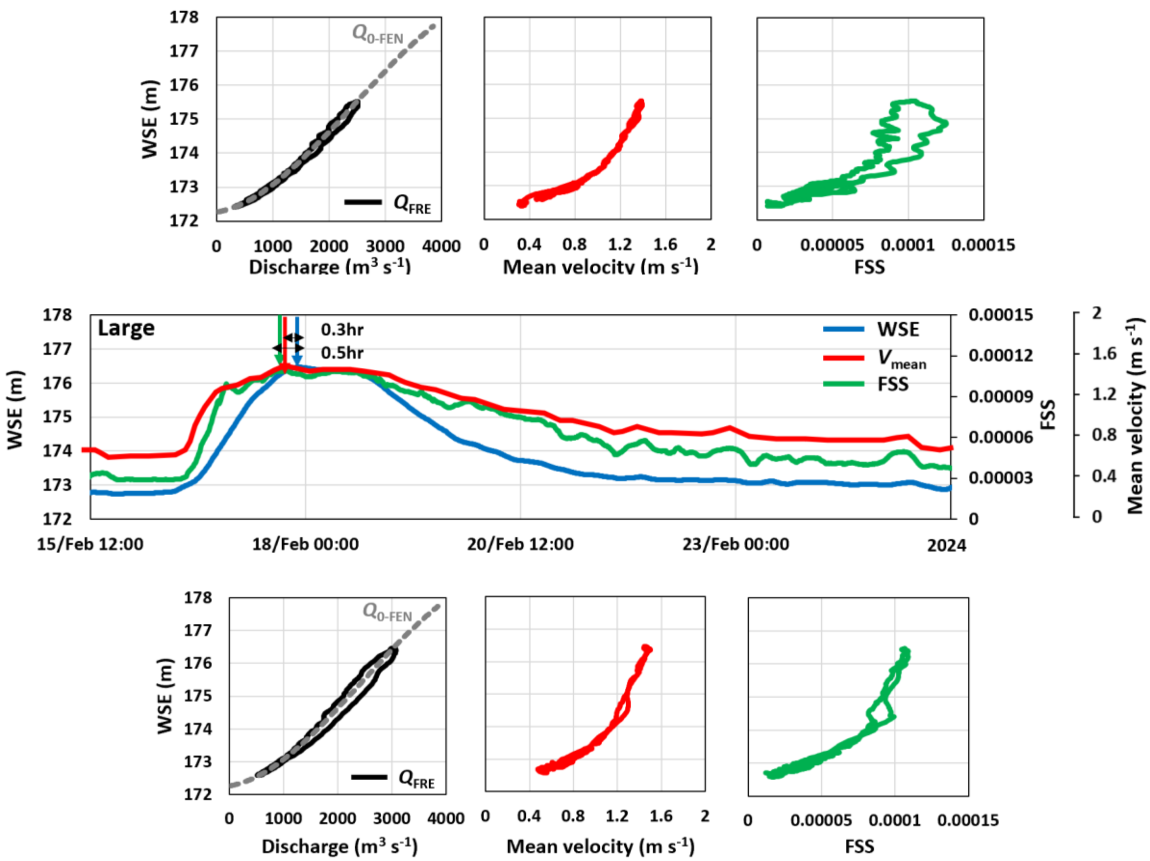

Figure 7. Dimensional graphs of the: 7a, 7c, and 7e time series for the main hydraulic variables for the three storm events identified in Figure 6a; and 7b, 7d, and 7f hysteretic loops between the stage and the main hydraulic variables for the same events.

The smaller phase lags and loop sizes plotted in these figures reveal that this site is only mildly affected by hysteresis, even for large flows. However, the plotted relationships illustrate that hysteresis is inherent in CVF, while its severity depends on the local site conditions (i.e., bed slope and of the severity of the propagating storms). Comparison of the graphs illustrated in Figures 4 and 7 and 5 and 8 reveals similar patterns for the phase lag between FSS and mean velocity peaks compared to the timing of depth peak and the presence of the loops albeit with much diminished values.

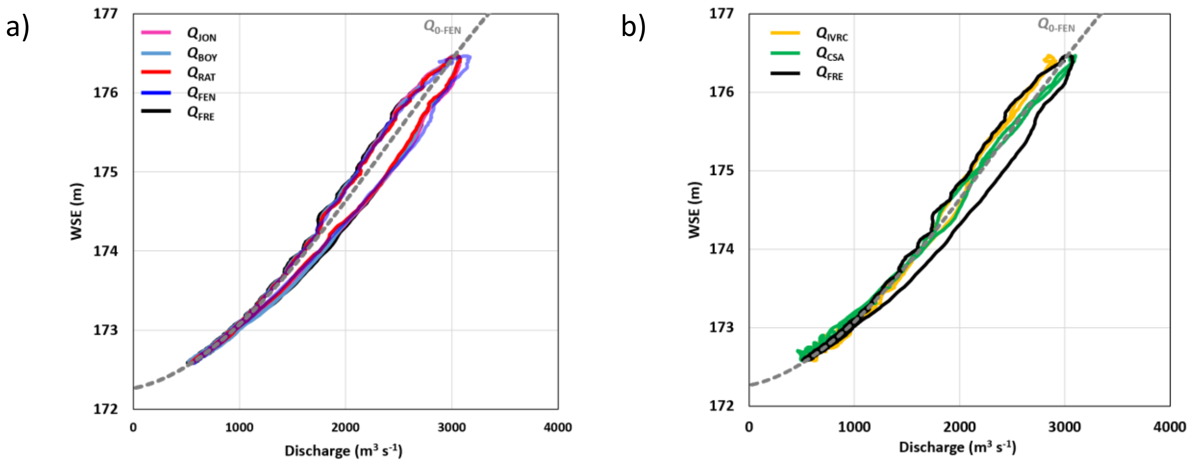

Figure 8. Performance of the alternative flow monitoring methods at Charleston site for: a) the HQRC correction methods listed in Table 1; and b) the stand-alone IVRC and CSA methods.

USGS # 03216070, Ironton (Ohio). The analysis at this site is focused on three storm events recorded at the station during the 2016-2023 period (see Figure 9a). Figure 9b overlays the maximum stage for the selected events over the gage site cross section. The loops for the actual flows are clearly visible in Figure 9b indicating gradual strengthening of hysteretic features as the event magnitude increases. The time-dependent and time independent representation of the relationships among the measured variables are plotted in Figure 10.

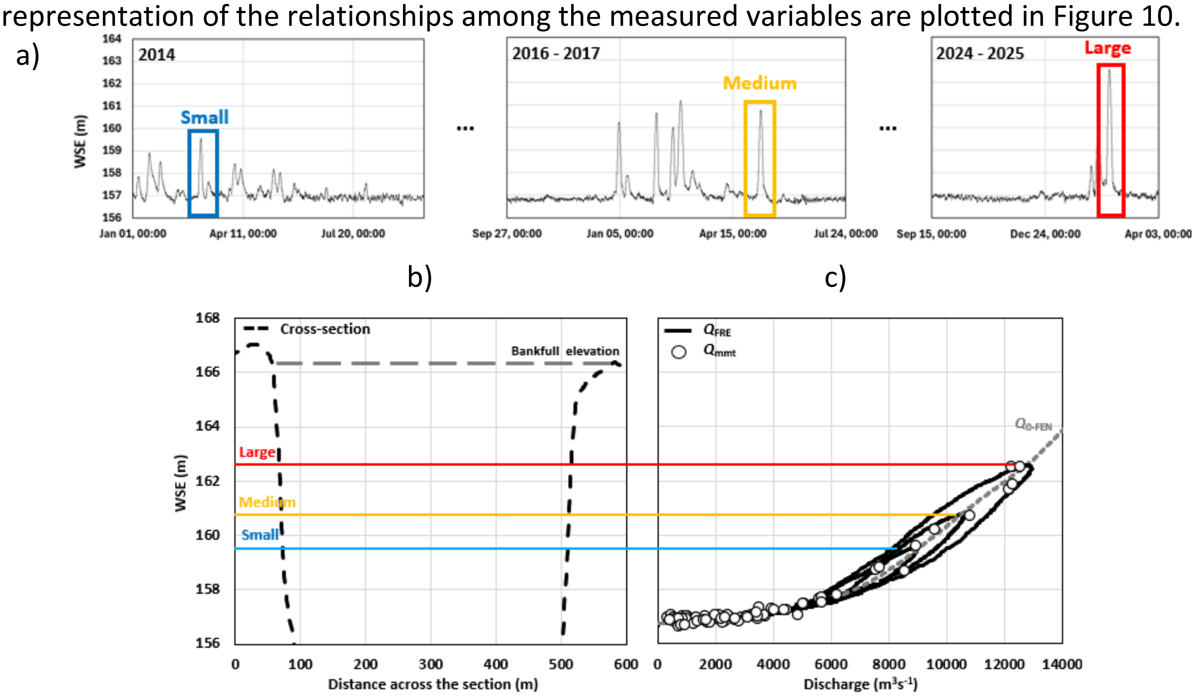

Figure 9. Basic analysis elements for the Ironton station: a) discharge time series for the 2016-2023 analysis period; b) river cross-section and maximum stages for analyzed storm events; and c) reference HQRC for the station (***$Q_{0\text{-}FEN}$***) and the trace of the actual flows estimated with ***Q_{FRE}*** correction method.

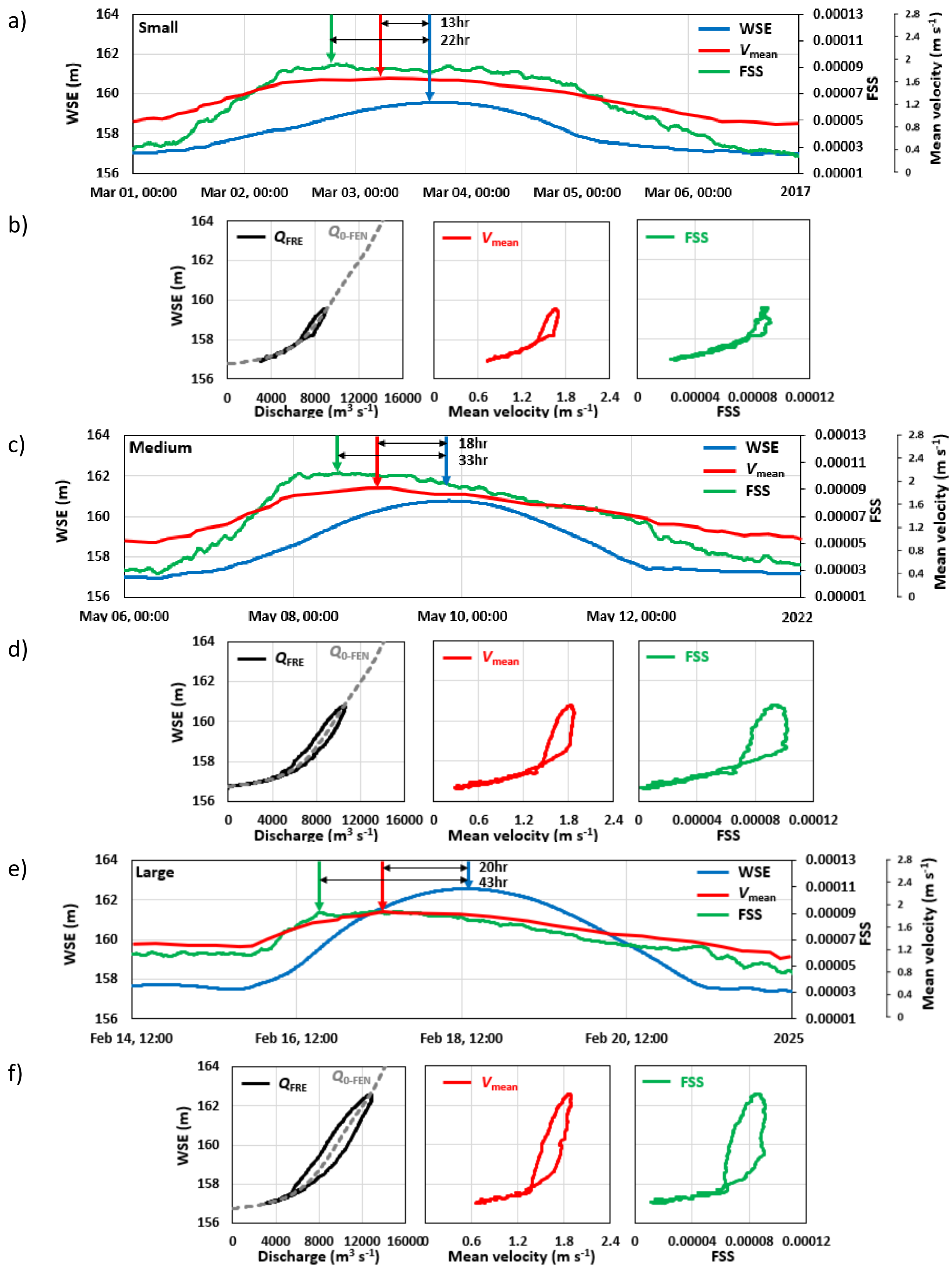
a)
Small
13hr
22hr
WSE
V_{mean}
FSS
WSE (m)
FSS
Mean velocity (m s-1)
Mar 01, 00:00
Mar 02, 00:00
Mar 03, 00:00
Mar 04, 00:00
Mar 05, 00:00
Mar 06, 00:00
2017
b)
Q_{FRE}
$Q_{0\text{-}FEN}$
Discharge (m3 s-1)
Mean velocity (m s-1)
c)
Medium
18hr
33hr
May 06, 00:00
May 08, 00:00
May 10, 00:00
May 12, 00:00
2022
d)
e)
Large
20hr
43hr
Feb 14, 12:00
Feb 16, 12:00
Feb 18, 12:00
Feb 20, 12:00
2025
f)

Figure 10. Dimensional graphs of the: 10a, 10c: and 10e time series for the main hydraulic variables for the three storm events identified in Figure 9a; and 10b, 10d and 10f: hysteretic loops between the stage and the main hydraulic variables for the same events.

Given that this site is located on the smallest bed slope value among the analyzed sites, it is anticipated that it displays the most prominent hysteretic features. The expected trends in the phasing of the variables are well illustrated by increased lags between the peaks of the FSS and index velocity with respect to stage peak timing in Figures 10a, 10c, and 10e. Similarly, the size of the loops among the measured variables increases in response to stronger propagating waves (see Figures 10b, 10d, and 10f). The 43 hours difference between FSS and stage shown in Figure 9e is the largest lag among the sites and represents a sufficient time interval to use this lag for forecasting purposes as discussed in Muste et al. (2022b). Overall, the plots in Figure 9 illustrate the close connection between the phase lag magnitude and the size of the looped ratings and the gradual increase of both hysteretic indicators with the storm event magnitude.

The level of performance for various monitoring methods is illustrated in Figure 11. It appears that the five HQRC correction methods listed in Table 1 perform satisfactory compared $\boldsymbol{Q_{FRE}}$, the reference method considered for the actual flows. Figure 11b compares $\boldsymbol{Q_{FRE}}$ with the multivariate streamflow methods that acquire an additional dynamic variable (i.e., free-surface slope or index velocity) to the stage measurements. The latter plots show that the $\boldsymbol{Q_{CSA}}$ data is in closer agreement with $\boldsymbol{Q_{FRE}}$ compared to $\boldsymbol{Q_{IVRC}}$ data. It is worth mentioning that $\boldsymbol{Q_{CSA}}$ and $\boldsymbol{Q_{IVRC}}$ data are completely independent of the HARC Q_0 data while the $\boldsymbol{Q_{FRE}}$ data is built on them.

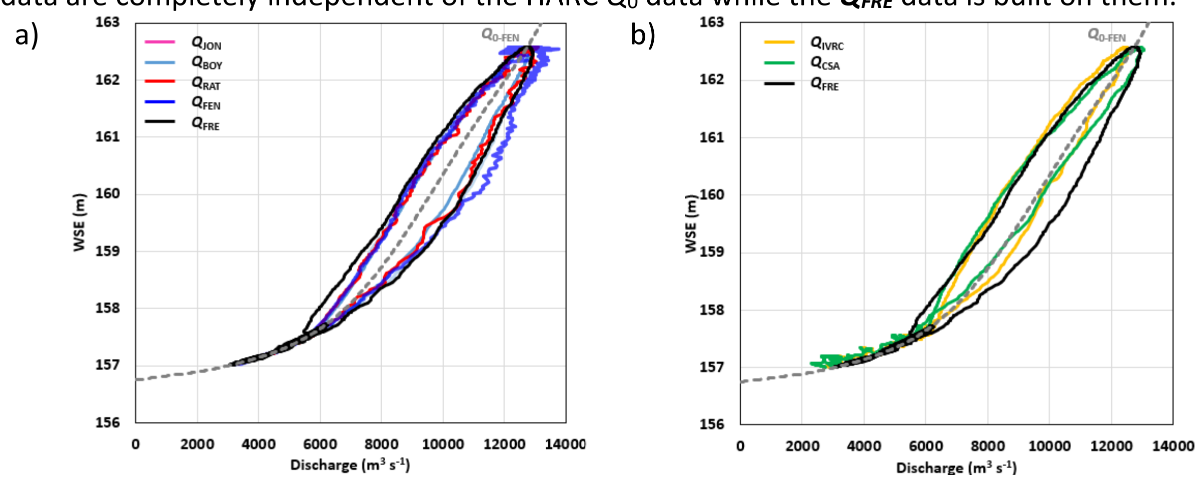

Figure 11. Performance of the alternative monitoring methods at Ironton site for: a) the HQRC correction methods listed in Table 1; and b) the stand-alone IVRC and CSA methods.

5 Discussion

The visualization of the selected HQRC corrections (i.e., Jones, Boyer, Rátky, and Fenton) and multi-variate monitoring methods (i.e., index-velocity and continuous slope area) applied at the three selected USGS operational gaging stations highlights their capabilities to replicate actual flow dynamics during gradually varied flows. The experimental evidence shows that actual flows consistently depart from the simple HQRC rating, The absolute values of the DRL and DFL differences for the largest events at each test site are illustrated in Table 3, using notations provided in Figure 2d.

Inspection of the numerical values shown in Table 3 allows to observe that the DRL absolute values across the analyzed methods range between 11 and 46% for the most severely hysteresis-affected site (Chattahoochee) and between 3 and 12% for the mildest hysteresis-affected site (Charleston). The DFL differences range between 5 and 23% for Chattahoochee and from 6 to 7% for Charleston. Notable, similar analysis conducted at Henry gaging station in Illinois (USGS # 0558300) displayed absolute differences of 65% for DRL and 18% for DFL (Muste et al., 2022a). The absolute value for the size of the actual flow loop is obtained by adding DRL and DFL deviations. Although the duration of the highest differences between actual flows and the HQRC records is typically short (e.g., of the order of several hours in in large rivers), these flow magnitudes are can trigger abrupt local changes in river morphology (e.g., bank failures, vegetation washout) and affect the status of the aquatic habitat (by distressing the aquatic life).

Similar observations can be made about the average values of the DRL and DFL over the looped areas (see also Figure 2d). An important consequence of the areal DRL and DFL differences from HQRC rating is that if the two areas are not equal, the estimation of loads for water constituents transported by the flow (e.g., suspended sediment, water quality pollutants) would yield different results. The hysteresis effect on the transport of water constituents is currently understudied because most of the load calculations are made using the simple HQRC that does not account for the flow variable hysteresis.

Table 3. Quantification of the departure of the actual flow indicated by $\boldsymbol{Q_{FRE}}$ from the simple HQRC rating, $\boldsymbol{Q_0}$ for the largest storm event analyzed at the analyzed gage sites

Method	Atlanta (Chattahoochee River, GA)				Charleston (Kanawha River, WV)				Ironton (Ohio River, OH)			
	Difference Rising (DRL) %		Difference Falling (DFL) %		Difference Rising (DRL) %		Difference Falling (DFL) %		Difference Rising (DRL) %		Difference Falling (DFL) %	
	Largest	Average	Largest	Average	Largest	Average	Largest	Average	Largest	Average	Largest	Average
Q_0 - Fenton (2018)	-	-	-	-	-	-	-	-	-	-	-	-
Jones	31	10	14	6	10	6	6	2	13	4	9	5
Boyer	11	4	5	2	11	6	6	3	8	3	8	4
Rátky	18	6	8	4	10	5	6	2	12	4	9	4
Fenton (2001)	36	11	13	6	11	6	6	2	17	6	10	5
Index-velocity	-	-	-	-	3	3	6	3	6	2	12	7
CSA	46	23	23	12	4	3	6	1	8	3	14	6
Fread	35	14	16	9	12	7	7	3	12	5	13	7

Table 4 evaluates the effectiveness of individual HQRC alternatives methods using $\boldsymbol{Q_{FRE}}$ as reference for comparison. About 80% of the average differences between the DRL and DFL reported values are below 5%, indicating that any of the methods provide a good monitoring alternative. While more comparison would be desirable for definitive conclusions, the present analysis indicates that the best overall performance among the tested methods is demonstrated by the Fenton and Rátky, while the least performant are Boyer and CSA. Another insight offered by the data is that the performance of the alternative method is site- and event-dependent, displaying different efficiencies for different sites and increased differences for the larger events.

Table 4. Comparison of alternative monitoring methods using $\boldsymbol{Q_{FRE}}$ as reference

Method	Atlanta Chattahoochee River, GA)				Charleston (Kanawha River, WV)				Ironton (Ohio River, OH)			
	Difference Rising (DRL) %		Difference Falling (DFL) %		Difference Rising (DRL) %		Difference Falling (DFL) %		Difference Rising (DRL) %		Difference Falling (DFL) %	
	Largest	Average	Largest	Average	Largest	Average	Largest	Average	Largest	Average	Largest	Average
Fread	-	-	-	-	-	-	-	-	-	-	-	-
Jones	16	8	10	5	4	1	2	1	4	1	9	2
Boyer	20	11	15	6	2	1	2	1	4	2	9	3
Rátky	17	9	13	5	5	2	3	1	7	2	8	3
Fenton (2001)	16	8	10	5	6	2	4	1	7	2	8	3
Index-velocity	-	-	-	-	14	9	9	3	9	4	13	3
CSA	16	8	10	5	21	7	6	2	12	5	9	2

The results presented in Section 4 offer a wealth of information on various aspects of GVF hysteresis as a stand-alone process and on issues associated with its accurate capture during storm propagation. These aspects are substantiated by the synoptic plots shown in Figure 12 for the largest events at each gaging site. The measured and estimated hydraulic variables in this figure are plotted in non-dimensional coordinates to enable cross-site and event comparisons.

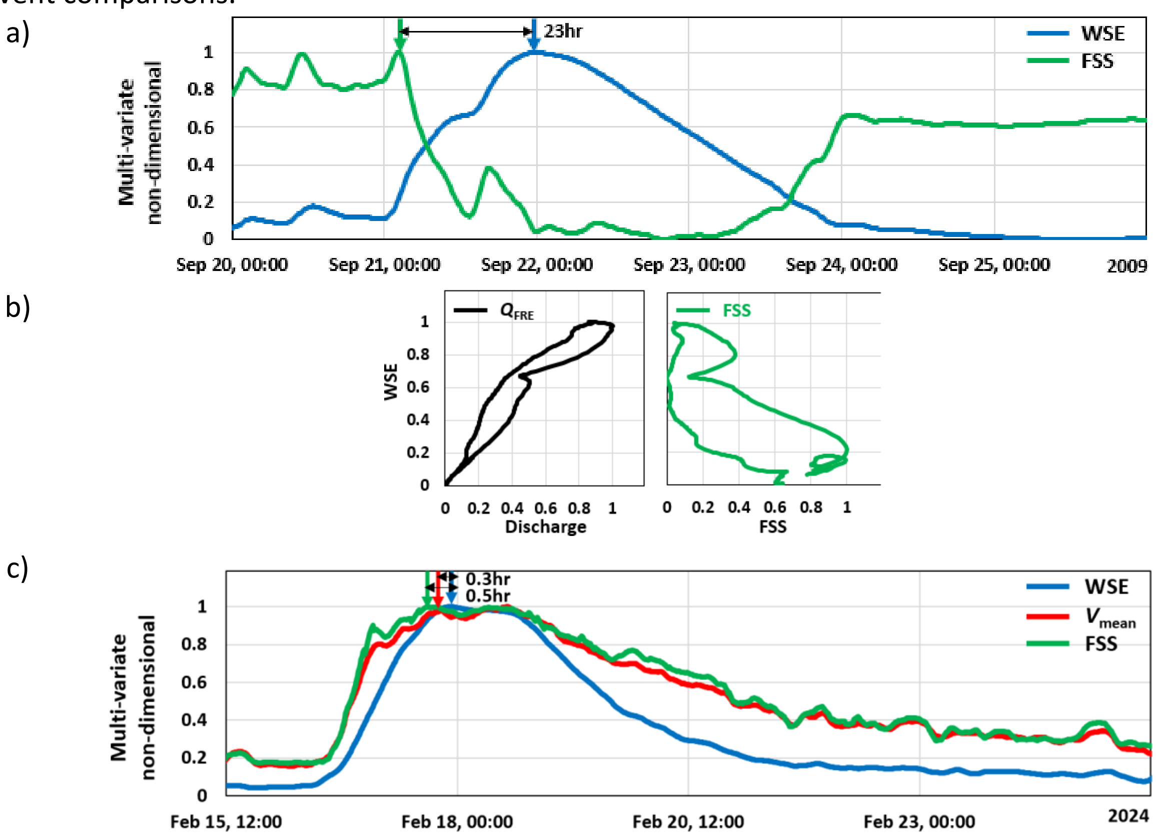

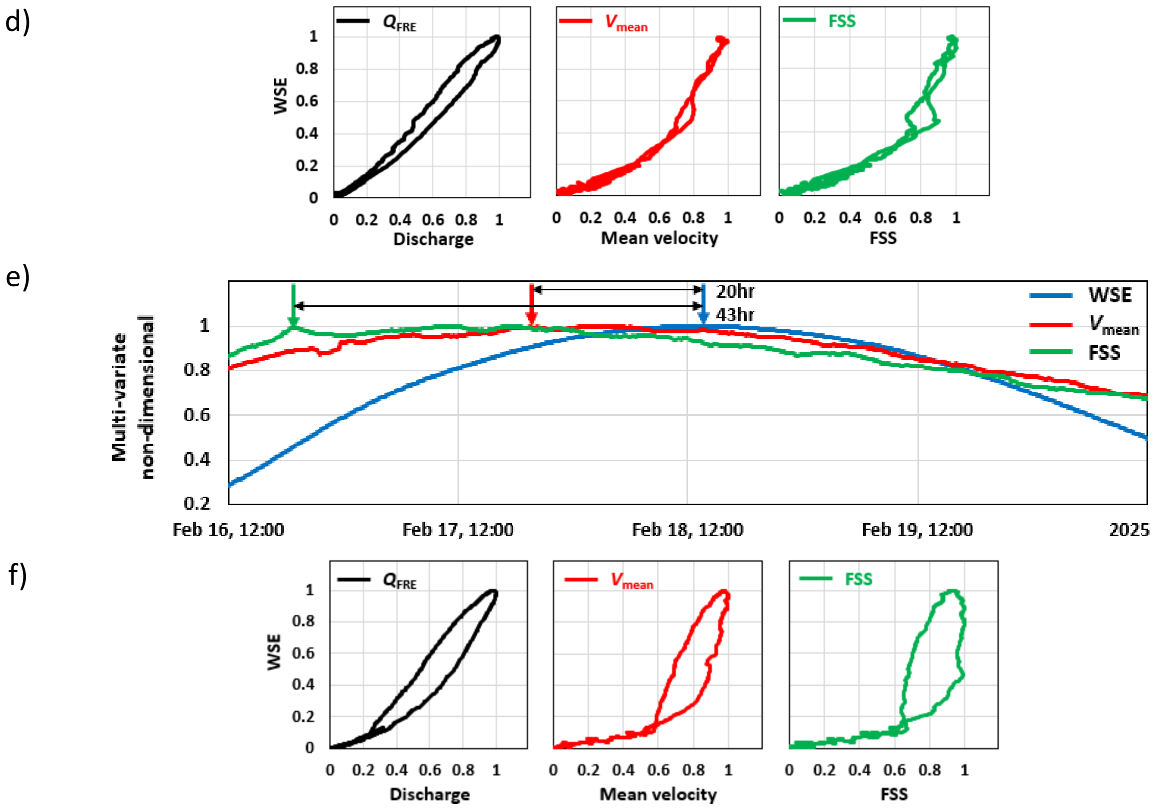

Figure 12. Non-dimensional representation of the phasing and loops among the measured hydraulic variables for the largest events analyzed at the study sites: a) b) Chattahoochee gaging station; c) d) Charleston gaging station; and e) f) Ironton gaging station.

A cursory inspection of the plots and Table 3 and Figure 12 reveals that the Charleston site is weakly hysteretic (with most of the DRL and DFL average differences lower than 5%), hence using the HQRC can be considered acceptable. The Chattahoochee and Ironton sites display DRL and DFL average differences larger than 5% and large time lags between variables' hydrographs peaks. These situations indicate the presence of mild to severe hysteresis effects requiring HQRC replacement with alternative methods.

Another notable feature in Figure 12 concerns the shape of the FSS time series. The common aspect of all the FSS traces is that they are starting and ending with quasi-equal values before and after the storm, and the maximum FSS values preceded the peaks of the other measured hydraulic variables, as indicated in the conceptual Figure 2e. However, the shape of the FSS trace for Chattahoochee differs from those for Charleston and Ironton. The FSS trace for Chattahoochee (Figure 12a) displays a sudden drop followed by a quick recovery during the storm propagation. This feature is not present at the other sites (see Figures 12c and 12e) where the shape of the FSS trace is similar for all the measured hydraulic variables. The difference in the shape of the FSS trace for the three test sites reveals an issue associated with data acquisition rather than reflecting a physical flow feature related to hysteresis.

The above-mentioned difference in FSS shapes is explained with numerical simulation results obtained by House et al. (2025b) at a hysteretic site on a large river (USGS #0558300 at

Henry, IL). Figure 13a visualizes FSS values sampled from the simulation outcomes at this station and at another hypothetical sampling point located 0.3, 1.8, and 12 km downstream. It can be noted that the larger the distance between the sampling stages, the lower the slope values (depicted graphically by the lower angle of the green segment inclination). Figure 13b illustrates the impact of using these spacings for reconstructing the FSS shape over time by continuously sampling the flood wave with the selected spacings. The FSS traces in this figure show that increasing the sampling distance used for FSS determination gradually flattens and distorts the FSS shape when graphed in time coordinates. From these considerations, it follows that the 1 km distance for determining FSS at the Chattahoochee site is sufficient to accurately reconstruct its shape (see Figure 12a), while the 6.5 km distance for the Charleston and Ironton sites (see Figures 12c and 12e) distorts the expected shape of the FSS time series. Notably, the estimation of the FSS with improper sampling distance have an impact of the location of the FSS peak compared to the stage peak.

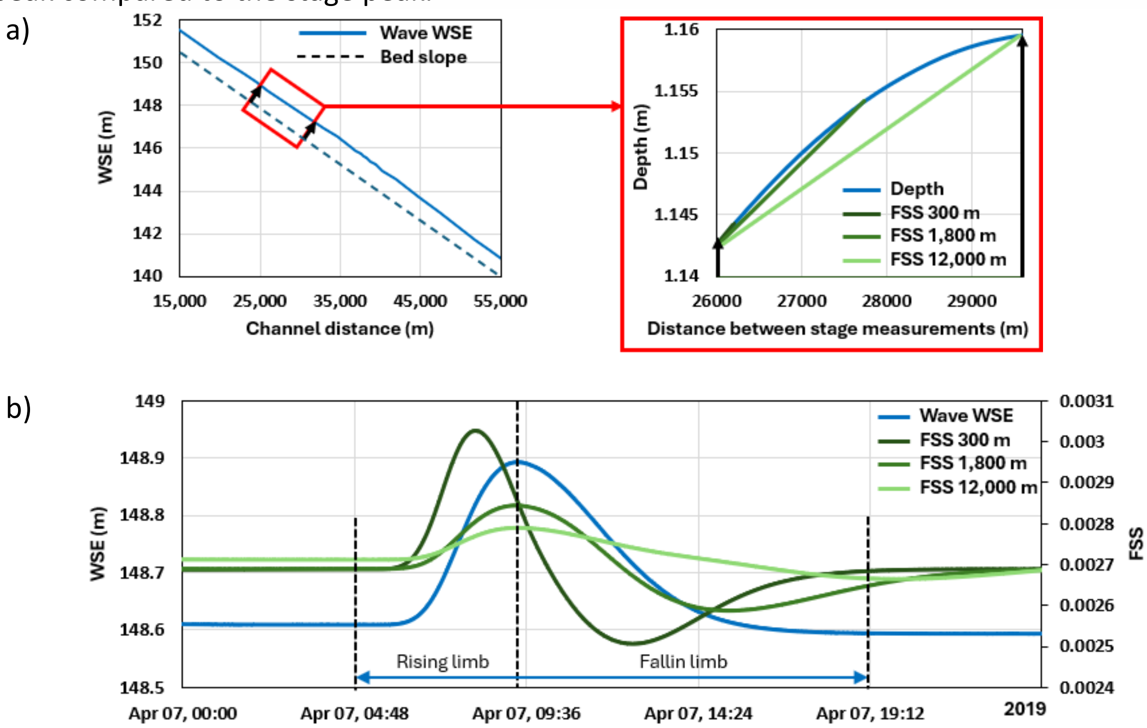

Figure 13. Impact of the sampling distance magnitude on the accuracy of the FSS time series shape: a) result of instantaneous FSS determination with various spacings between stations; b) the impact of the FSS tracing in time with various sampling spacings

The published literature reports FSS estimates determined from stages acquired over a wide range of distances, from several tenths of meters (Smith et al., 2010) to tens of kilometers (e.g., Dottori et al., 2009; Schumann et al., 2010) without relating the quality of FSS determination with the sampling requirements. Lacking rigorous guidance, the distance between the stage sampling points is mostly guided by practical concern such as to obtain a measurabale stage fall that can be reliably measured by the instrumentation at hand. However, the issue of fulfilling proper spatial and temporal resolution requirements for accurately determining the actual shape of the FSS time series requires more attention as it is critical when the data is used for supporting calibration and validation of numerical models or for decision-making in real engineering problems.

The new experimental evidence presented in this study illustrates that the HQRC alternative methods successfully attempt to recover the flow dynamics lost by considering GVFs as piecewise uniform flows of various magnitudes, as assumed by HQRC construction. We acknowledge that the nine cases analyzed in this paper are not sufficient to draw definitive conclusions on the true performance of the alternative monitoring methods. However, the hysteretic features captured for each site and flow event align with analytical (e.g., Muste et al., 2017) and experimental findings of previous analyses (e.g., Holmes, 2016) and those conducted by the present authors (Lee & Muste, 2017; Muste et al., 2019; Muste et al., 2020; Muste et al., 2022a, 2022b; Muste et al., 2024; Muste et al., 2025). The good agreement with previous studies on hysteretic flows offers confidence that the performance analysis carried out in this study is relevant for other sites with similar ranges for the geomorphic, hydrologic, hydraulic conditions.

To integrate this study into the decision-making process, Figure 14 provides a sequence of steps accounting for hydraulic and economic factors to determine whether an existing HQRC station is sufficient for the station or an alternative approach should be adopted to account for GVF effects. The hydraulic factor is encapsulated in the “hysteresis diagnostic” formula that enables to anticipate the wave type developing for specific sites and runoff events based on prior streamflow data recorded at the stations (Muste et al., 2020). Lee (2013) identified about a dozen of such formula developed by previous studies focused on fluvial wave types. Based on the outcomes of the hysteresis diagnostic (i.e., anticipating the presence of kinematic, diffusive or dynamic type waves for the large events propagating through the site), the monitoring method protocol can either be maintained in its current configuration or modified with interventions to meet higher quality specifications for the recorded streamflow data. The selection of the suitable alternative monitoring approach for a specific station should be decided by a robust cost-benefit analysis that weighs the quality benefits against the costs required to upgrade the station. This decision-making process is applicable to existing and planned monitoring stations.

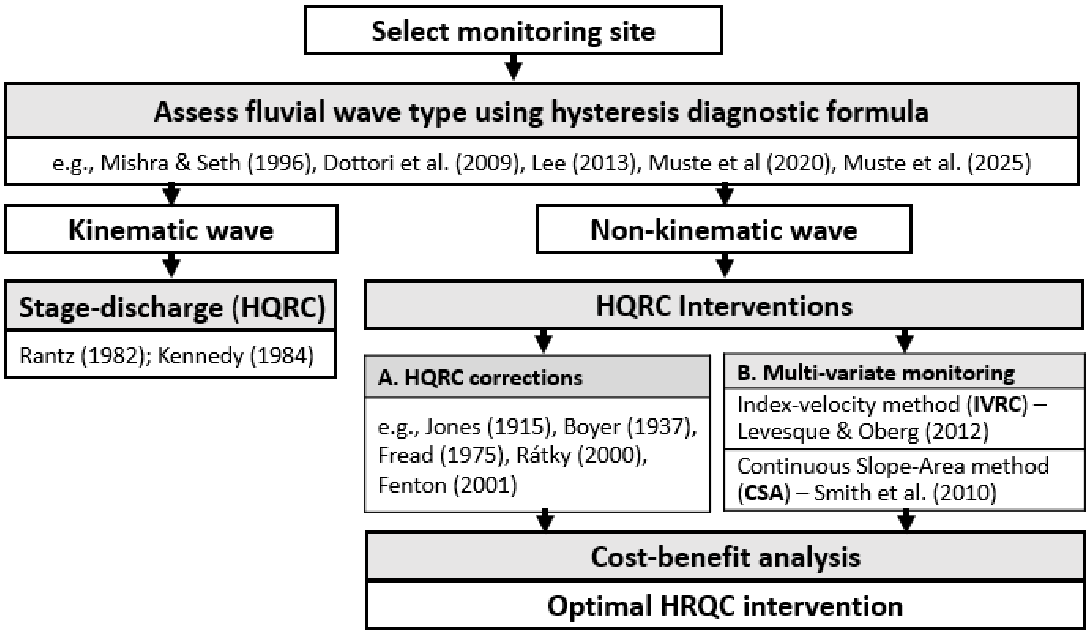

Figure 14. Decision-making tree for assessing the need for maintain or replace a HQRC gaging station with an improved configuration for the monitoring protocol

Given that the errors in GVF streamflow data produced by HQRC ratings are site specific and vary for each event, a parsimonious and defensible approach in ascertaining data uncertainty would be to apply one of the HQRC alternative methods and assess its performance in a similar manner as reported in Tables 3 and 4. Assuming that the performance analysis of the alternative method is applied to the largest hydrological events passing through the gaging site, its results can be deemed as providing the largest uncertainty in the HQRC rating for the specific gaging location. A more robust uncertainty analysis approach would be to repeat the analysis for a several flows over the range of possible flows encountered at the site and use the analyses outcomes to develop an “uncertainty rating“ that will provide uncertainty values associated with various flow magnitudes. Given that high cost associated with conducting such analyses, the uncertainty rating can be constructed by temporarily deploying the most economically feasible method available to the local hydrometric agency and subsequently associate the uncertainty estimates to the existing HQRC. The analysis may be repeated over time if any of the other sources of errors are deemed to substantially affect the existing HQRC rating performance.

6 Conclusion

The new experimental evidence extracted from public data reveals the potential of the vast amount of data archived in online resources to document understudied river behavior from various perspectives. One of these perspective is to exploring these resources as a means for testing streamflow monitoring protocols. The exploration can substantiate evidence of the poor replication of gradually varied flows by Manning’s equation (the central analytical guide for HQRC rating) applied to piecewise steady and uniform flows, and the necessity to more adequately capture the important phenomenon of stage-discharge hysteresis, which is not currently substantiated at USGS gaging stations.

In an attempt to fill gaps in assessing the quality of the HQRC-derived streamflow data, this paper examines one of the most pervasive factors affecting the accuracy of streamflow data that is not captured by conventional stage-discharge ratings: hysteresis. While hydrometric agencies recognize these limitations and apply corrections, assessing their effectiveness is still lagging, leaving hysteresis-induced errors unaddressed. The analysis of the experimental evidence presented in this paper contributes to the evaluation of HQRC performance in GVFs through several new insights:

- Streamflow data reported at gaging sites with stage-discharge ratings obscure the inherent hysteretic effects of gradually varied flow, which are often larger than the 5% uncertainty tacitly assumed for streamflow time series. This operational omission in streamflow monitoring is especially critical on the rising limb of the hydrographs in flood-prone lowland areas where hysteresis can be severe.
- Conventional correction methods for stage-discharge and multi-variate monitoring methods reconstruct the traces of variables in gradually varied flow with high confidence, including flows exceeding the bankful stage.
- Stage-discharge correction methods that account for more terms in the gradually varied flow governing equations (e.g., Fread) perform systematically better than those using simplifying assumptions (e.g., Boyer, Jones, and CSA).
- Our experimental evidence reinforces previous findings that measuring the FSS is critical in capturing fluvial wave dynamics. (e.g., Fenton, 2001; Aricò et al., 2009; Dottori et al., 2009)
- By including the FSS as an additional flow dynamic variable and information on the channel cross-section into the monitoring protocol for every gauged site can greatly enhance the understanding of the site-specific issues related to rating curves.
- Fulfilling spatial and temporal sampling requirements is critical for accurate FSS estimation, which contrasts with current hydrometric practices.

Given that our understanding the hysteresis behavior in GVFs is still incomplete, re-examining the underlying physics of unsteady nonuniform flows remains a priority for improving the accuracy of the operational monitoring methods and for supporting the modeling of these flows for practical and scientific purposes. It is hoped that the experimental evidence illustrated in this study sheds light on less understood aspects of gradually varied flows and reveals subtle features of the non-unique relationships among the hydraulic variables.

Acknowledgments

The first author acknowledges the support provided by the National Science foundation award NSF- EAR- HS 2139649. The second author was funded by the National Oceanic and Atmospheric Administration (NOAA), awarded to the Cooperative Institute for Research on Hydrology (CIROH) through the NOAA Cooperative Agreement with The University of Alabama, NA22NWS4320003. The third author acknowledges the support provided by the Korea Environment Industry & Technology Institute (KEITI) through the Research and Development on the Technology for Securing Water Resources Stability in Response to Future Change Program, funded by the Korea Ministry of Environment (MOE) (RS-2024-00336020). We greatly appreciate the dialogue and support of the US Geological Survey researchers A. Gotvald and T. Kenney. The additional data provided by the USGS hydrologists Bob Sobczak and Christopher A. Smith, Jeremy S. White, Nathan Truax, Timothy Shawn LeMaster are also gratefully acknowledged.

References

Alabbad, Y., Yildirim, E., & Demir, I. (2023). A web-based analytical urban flood damage and loss estimation framework. Environmental Modelling & Software, 163, 105670.

Aricò, C., Nasello, C., & Tucciarelli, T. (2009). Using unsteady-state water level data to estimate channel roughness and discharge hydrograph. Advances in Water Resources, 32(8), 1223–1240. https://doi.org/10.1016/j.advwatres.2009.05.001

Boyer, M.C. (1937). Analysis of Methods of Adjusting Stage and Discharge for Measurements During Changing Stage. Water Resources Bulletin, unpublished manuscript of the Water-Resources Branch of the U.S. Geological Survey, 192-200

Chow, V. T., 1959, Open-Channel Hydraulics, McGraw-Hill Book Co., New York, NY.

Cikmaz, B. A., Yildirim, E., & Demir, I. (2025). Flood susceptibility mapping using fuzzy analytical hierarchy process for Cedar Rapids, Iowa. International journal of river basin management, 23(1), 1-13.

Coxon, G., J. Freer, I. K. Westerberg, T. Wagener, R. Woods, and P. J. Smith (2015), A novel framework for discharge uncertainty quantification applied to 500 UK gauging stations, Water Resour. Res., 51, 5531–5546, doi:10.1002/2014WR016532

Dalrymple, T. and Benson, M. A. (1967). Measurement of peak discharge by the slope-area method: U.S. Geological Survey Techniques of Water-Resources Investigations, book 3, chap. A2, p. 12.

Demir, I., Xiang, Z., Demiray, B., & Sit, M. (2022). Waterbench: a large-scale benchmark dataset for data-driven streamflow forecasting. Earth System Science Data Discussions, 2022, 1-19.

Domanski, M., Holmes, R.R., Jr. and Heal, E.N. (2022), Dynamic rating method for computing discharge from time-series stage data: U.S. Geological Survey Open-File Report 2022–1031, 48 p., https://doi.org/10.3133/ofr20221031

Domanski, M.M., Holmes, R.R., Jr., Heal, E.N., and Knight, T.M. (2025). Dynamic rating method for computing discharge and stage from time-series data: U.S. Geological Survey Scientific Investigations Report 2024–5129, 92 p., https://doi.org/10.3133/sir20245129

Dottori, F., Martina, L.V. and Todini, E. (2009). A Dynamic Rating Curve Approach to Indirect Discharge Measurements. Hydrology. Earth Syst. Sci, 13, 847-863.

Fenton, J. D. (2001)., in Proc. Conf. on Hydraulics in Civil Engng, 28-30 Nov., Inst. Engnrs, Aust., Hobart, pp. 309-317.

Fenton, J.D. (2018). On the generation of stream rating curves, J Hydrology, 564, pp. 748-757, https://doi.or2/10.l 016/i.ihvdrol.2018.07.025

Ferrick, M. G. (1985). Analysis of river wave types. Water Resources Research 21(2): 209-220.

Fread, D. L. (1975). Computation of stage-discharge relationship affected by unsteady flow, Water Resources Bulletin, 11(2), 429–442.

Gharari, S., Whitfield, P.H., Pietroniro, A., Freer, J., Liu, H. and Clark, M.P. (2024). Exploring the provenance of information across Canadian hydrometric stations: implications for discharge estimation and uncertainty quantification, Hydrol. Earth Syst. Sci., 28, pp.4383-4405, doi.org/10.5194/hess-28-4383-2024

Graf, W. and Qu, Z. (2004). Flood hydrographs in open channels Proceedings of the Institution of Civil Engineers-Water Management, 157(1), pp. 45–52, doi.org/10.1680/wama.2004.157.1.45

Henderson, F.M. (1966). Open Channel Flow. Macmillan Series in Civil Engineering; Macmillan Company: New York, NY, USA, p. 522.

Herschy, R.W (2009). Streamflow measurement, 3rd ed. CRC Press, doi.org/10.1201/9781482265880

Holmes, R.R. (2016). River rating complexity. In Proceedings River Flow Conference; Taylor & Francis Group: St. Louis, MO, USA, ISBN 978-1-138-02913-2.

House, E., Meselhe, E., Muste, M., & Demir, I. (2025). Streamflow hysteresis analysis through a deep dive budget of the St Venant momentum terms. EarthArXiv. https://doi.org/10.31223/X5W44C

House, E., Kim, K., Muste, M., Meselhe, E., & Demir, I. (2025). Back to basics: On the proper determination of free-surface slope in gradually varied open channel flows. EarthArXiv. https://doi.org/10.31223/X50X5M

ISO (2020). Hydrometry — Measurement of liquid flow in open channels — Determination of the stage–discharge relationship, International Organization for Standardization, ISO 18320(en), Geneva, Switzerland.

Jones, B. E. (1915). A method of correcting river discharge for a changing stage, U.S. Geological Survey Water Supply Paper, 375-E, 117–130.

Kennedy, E. (1984). Discharge ratings at gaging stations: US Geological Survey Techniques of Water-Resources Investigations, book 3, chap. A10, 59p.

Kiang, J. E., Gazoorian, C., McMillan, H., Coxon, G., Le Coz, J., Westerberg, I. K., et al. (2018). A comparison of methods for streamflow uncertainty estimation. Water Resources Research, 54, https://doi.org/10.1029/2018WR022708

Krajewski, W. F., Ghimire, G. R., Demir, I., & Mantilla, R. (2021). Real-time streamflow forecasting: AI vs. Hydrologic insights. Journal of Hydrology X, 13, 100110.

Kumar, A. (2011). Stage-Discharge Relationship. In: Singh, V.P., Singh, P., Haritashya, U.K. (eds) Encyclopedia of Snow, Ice and Glaciers. Encyclopedia of Earth Sciences Series. Springer, Dordrecht. doi.org/10.1007/978-90-481-2642-2_537

Lee, K. (2013). Evaluation of methodologies for continuous discharge monitoring in unsteady open-channel flows [Doctoral dissertation, The University of Iowa]. https://ir.uiowa.edu/etd/5012

Lee, K., Muste, M. (2017). “Refinement of Fread’s Method for Improved Tracking of Stream Discharges during Unsteady Flows,” J. Hydraulic Engineering, doi: 10.1061/(ASCE)HY.1943-7900.0001280

Levesque, V. A. and Oberg, K. A. (2012). Computing discharge using the index velocity method: US Department of the Interior, US Geological Survey.

McMahon, T.A. and Peel, M.C. (2019) Uncertainty in stage–discharge rating curves: application to Australian Hydrologic Reference Stations data, Hydrological Sciences Journal, 64:3, 255-275, doi/10.1080/02626667.2019.1577555

McMillan, H., Seibert, J., Petersen-Overleir, A., Lang, M., White, P., Snelder, T., et al. (2017). How uncertainty analysis of streamflow data can reduce costs and promote robust decisions in water management applications. Water Resources Research, 53, doi.org/10.1002/2016WR020328, pp. 5220–5228

Mishra, S.K. and Seth, S.M. (1996). Use of hysteresis for defining the nature of flood wave propagation in natural channels. Hydrological Sciences-Journal-des Sciences Hydrologiques 41(2), 153–170.

Moramarco, T., Pandolfo, C. and Singh, V. P. (2008). Accuracy of kinematic wave and diffusion wave approximations for flood routing. II: Unsteady analysis.” J. Hydrol. Eng., 13(11), 1089–1096.

Moussa, R., & Bocquillon, C. (1966). Criteria for the choice of flood-routing methods in natural channels, J. Hydrology 186, pp. 1-30.

Muste, M., Cheng, Z., Firoozfar, A. R., Tsai, H.-W., Loeser, T., & Xu, H. (2016). Impacts of unsteady flows on monitoring stream flows, River Flow Conference, St Louis, MO.

Muste, M., Lyn, D. A., Admiraal, D., Ettema, R., Nikora, V., & Garcia, M. H. (2017). Experimental hydraulics: Methods, instrumentation, data processing and management: Volume I: Fundamentals and methods. CRC Press.

Muste, M., Bacotiu, C. and Thomas, D. (2019). Evaluation of the slope-area method for continuous streamflow monitoring. Paper presented at the Proceedings of the 38th World Congress, Panama City, Panama.

Muste, M., Lee, K., Kim, D., Bacotiu, C., Rojas Oliveros, M., Cheng, Z. and Quintero, F. (2020). “Revisiting Hysteresis of Flow Variables in Monitoring Unsteady Streamflows” State-of-the-art Paper Series, Journal of Hydraulic Research; 58(6), pp. 867-887, doi.org/10.1080/00221686.2020.1786742

Muste, M.; Kim, D.; Kim, K. (2022a) Insights into flood wave propagation in natural streams as captured with Acoustic Profilers at an Index-Velocity gaging station, Water, 14, 1380.

Muste, M., Kim, D. and Kim, K. (2022b). A flood-crest forecast prototype for river floods using only in-stream measurements, Communications Earth & Environment, doi.org/10.1038/s43247-022-00402-z

Muste, M., Kim, K. and Demir, I. (2024). Stage-discharge Ratings in Unsteady Flows: Corrections, Improvements, Replacements, AGU Fall Meeting, December 9-13, 2024, Washington DC.

Muste, M., Kim, K., Kim, D. and Fleit G. (2025). Decoding the hysteretic behavior of hydraulic variables in lowland rivers with multivariate monitoring approaches, Hydrological Processes, Special Issue on “Hydrological processes in lowlands and plains”, doi: 10.1002/hyp.70008

Petersen-Øverleir, A. (2006). Modelling stage–discharge relationships affected by hysteresis using the Jones formula and nonlinear regression, *Hydrological Sciences Journal,* 51(3), pp. 365-388.

Petersen-Øverleir, A., A. Soot, and T. Reitan (2009), Bayesian Rating Curve Inference as a Streamflow Data Quality Assessment Tool, Water Resour. Manage., 23, 1835–1842, doi:10.1007/s11269-008-9354-5

Ponce, V.M. (1991). The kinematic wave controversy. J. Hydr. Engrg., ASCE, 117(4), 511–525.

Rantz, S.E. and others., 1982. Measurement and Computation of Streamflow. United States Geological Survey Water Supply Paper 2175, Vol 1, 2.

Rozos, E., Leandro, J. and Koutsoyiannis, D. (2022). Development of rating curves: Machine Learning vs. Statistical Methods. Hydrology, 9, doi.org/10.3390/hydrology910016

Rátky, I. (2000) Árvízi hurokgörbék közelítő számítása. Vízügyi Közlemények 82(2), pp. 232—261(in Hungarian).

Schmidt, A. R. (2002). Analysis of stage-discharge relations for open-channel flows and their associated uncertainties. PhD Thesis Dissertation, University of Illinois at Urbana-Champaign, IL.

Schmidt, A.R. and Garcia, M.H. (2003). Theoretical examination of historical shifts and adjustments to stage-discharge rating curves, ASCE World Water & Environmental Resources Congress, Philadelphia, PA.

Schumann, G., G. Di Baldassarre, D. Alsdorf, and P. D. Bates (2010), Near real-time flood wave approximation on large rivers from space: Application to the River Po, Italy, Water Resour. Res., 46, W05601, doi:10.1029/2008WR007672

Sermet, Y., Villanueva, P., Sit, M. A., & Demir, I. (2020). Crowdsourced approaches for stage measurements at ungauged locations using smartphones. Hydrological Sciences Journal, 65(5), 813-822.

Smith, C.F., Cordova, J.T., and Wiele, S.M. (2010). The continuous slope-area method for computing event hydrographs: U.S. Geological Survey Scientific Investigations Report 2010-5241, 37 p.

Stewart, A. M., Callegary, J. B., Smith, C. F., Gupta, H. V., Leenhouts, J. M., & Fritzinger, R. A. (2012). Use of the continuous slope-area method to estimate runoff in a network of ephemeral channels, southeast Arizona, USA, Journal of Hydrology, 472, pp. 148-158.

USGS (1994). A history of the Water Resources Branch, U.S. Geological Survey; Follansbee, R., Ed.; Volume I, from Predecessor Surveys to 30 June 1919; U.S. Geological Survey: Denver, CO, USA.

WMO (2010). Manual on stream gauging. Volume I: Fieldwork, WMO No.1064, World Meteorological Organization, Geneva, Switzerland.

Xiang, Z., Demir, I., Mantilla, R., & Krajewski, W. F. (2021). A regional semi-distributed streamflow model using deep learning. EarthArxiv, 2152. https://doi.org/10.31223/X5GW3V

Yen, B.C. (1973) Open-channel flow equations revisited, J Eng Mech Div., ASCE, 99, pp. 979–1009.

Yildirim, E., Just, C., & Demir, I. (2022). Flood risk assessment and quantification at the community and property level in the State of Iowa. International journal of disaster risk reduction, 77, 103106.